International Journal of
Molecular Sciences

MDPI

Article

Resilience in Long-Term Viral Infection: Genetic Determinants and Interactions

Candice Brinkmeyer-Langford [1,*], Katia Amstalden [1], Kranti Konganti [2], Andrew Hillhouse [2], Koedi Lawley [1], Aracely Perez-Gomez [1], Colin R. Young [1], C. Jane Welsh [1,3] and David W. Threadgill [2,4]

1 Department of Veterinary Integrative Biosciences, Texas A&M University, College Station, TX 77843, USA; kamstalden@cvm.tamu.edu (K.A.); koedilawley@tamu.edu (K.L.); aapg96@tamu.edu (A.P.-G.); cyoung@cvm.tamu.edu (C.R.Y.); jwelsh@cvm.tamu.edu (C.J.W.)
2 Texas A&M Institute for Genome Sciences and Society, Texas A&M University, College Station, TX 77843, USA; konganti@tamu.edu (K.K.); hillhouse@tamu.edu (A.H.); dwthreadgill@tamu.edu (D.W.T.)
3 Department of Veterinary Pathobiology, Texas A&M University, College Station, TX 77843, USA
4 Department of Molecular and Cellular Medicine, Texas A&M University, College Station, TX 77843, USA
* Correspondence: brinkmeyer@tamu.edu

Abstract: Virus-induced neurological sequelae resulting from infection by Theiler's murine encephalomyelitis virus (TMEV) are used for studying human conditions ranging from epileptic seizures to demyelinating disease. Mouse strains are typically considered susceptible or resistant to TMEV infection based on viral persistence and extreme phenotypes, such as demyelination. We have identified a broader spectrum of phenotypic outcomes by infecting strains of the genetically diverse Collaborative Cross (CC) mouse resource. We evaluated the chronic-infection gene expression profiles of hippocampi and thoracic spinal cords for 19 CC strains in relation to phenotypic severity and TMEV persistence. Strains were clustered based on similar phenotypic profiles and TMEV levels at 90 days post-infection, and we categorized distinct TMEV response profiles. The three most common profiles included "resistant" and "susceptible," as before, as well as a "resilient" TMEV response group which experienced both TMEV persistence and mild neurological phenotypes even at 90 days post-infection. Each profile had a distinct gene expression signature, allowing the identification of pathways and networks specific to each TMEV response group. CC founder haplotypes for genes involved in these pathways/networks revealed candidate response-specific alleles. These alleles demonstrated pleiotropy and epigenetic (miRNA) regulation in long-term TMEV infection, with particular relevance for resilient mouse strains.

Keywords: TMEV; resilience; collaborative cross; gene expression

Citation: Brinkmeyer-Langford, C.; Amstalden, K.; Konganti, K.; Hillhouse, A.; Lawley, K.; Perez-Gomez, A.; Young, C.R.; Welsh, C.J.; Threadgill, D.W. Resilience in Long-Term Viral Infection: Genetic Determinants and Interactions. *Int. J. Mol. Sci.* **2021**, *22*, 11379. https://doi.org/10.3390/ijms222111379

Academic Editors: Caterina Garone and Dario Brunetti

Received: 2 October 2021
Accepted: 20 October 2021
Published: 21 October 2021

1. Introduction

Theiler's murine encephalomyelitis virus, or TMEV, causes a variety of neurological sequelae in rodents depending on the genetic background of the host. TMEV infection has long been used as a model for virally induced demyelinating disease or epilepsy, but recent studies in our lab have revealed outcomes to TMEV infection much more nuanced and complex than any previously seen in mice. These outcomes are more similar to the range of effects seen in humans with viral infections. To characterize the spectrum of responses to TMEV, we use the Collaborative Cross, a resource of diverse mouse strains derived from a crossbreeding scheme including five common (A/J, C57BL/6J, 129S1/SvlmJ, NOD/ShiLtJ, NZO/HlLtJ) and three wild-derived (CAST/EiJ, PWK/Ph, and WSB/EiJ) inbred mouse strains. This crossbreeding "funnel" renders each CC strain genetically and phenotypically distinct, with the genetic diversity of an outbred population but the reproducibility of an inbred population [1,2]. We have also evaluated CC-RIX strains (recombinant inbred intercrosses) as additional sources of diversity [3].

Previous studies have identified genetic factors linked to TMEV resistance or susceptibility, with these responses defined in relation to TMEV-induced demyelinating disease or viral persistence [4–20]. In fact, TMEV infection outcome has been studied in one of the eight CC founder strains: the TMEV-resistant strain C57BL/6J. However, the complex genetic diversity among the CC mouse strains has allowed us not only to identify novel TMEV-induced phenotypes, but to identify and explore additional genetic factors contributing to these responses. We hypothesized that genetic factors also underlie novel outcomes of TMEV infection, particularly resilience.

By evaluating long-term TMEV infection in 19 CC strains, we observed outcomes ranging from seizures to weakness and paralysis. Similar to humans infected by a virus, each individual CC strain responded uniquely to TMEV infection. We did not find TMEV persistence to be a driving factor for disease severity in any phenotype evaluated. We also observed TMEV outcomes unlike any previously described in conventional mouse strains. In addition to classical TMEV resistance (defined here as evidence of TMEV clearance with mild clinical phenotypes in the chronic phase of infection), and susceptibility (evidence of TMEV persistence with severe clinical phenotypes during chronic phase), we also identified several CC strains with persistent TMEV infection but mild clinical signs of disease during the late chronic phase. We define such mice as "resilient" to TMEV infection.

In the current study, we performed RNA sequencing during the late chronic phase of TMEV infection to identify key factors determining the severity of neurological symptoms. We first evaluated gene expression in all TMEV-infected mice versus sham-infected mice, pooling all 19 CC strains to understand the overall effect of TMEV infection on gene expression, host genetic backgrounds notwithstanding. Next, we categorized individual CC strains based on similar TMEV responses (resistant, resilient, or susceptible), and characterized the genetic underpinnings distinguishing each category.

By comparing differentially expressed genes (DEGs) across different TMEV response categories, we identified genes and sequence variants which correlate with TMEV resistance and susceptibility, and—most importantly—with resilience. We also identified novel biomarkers for TMEV disease outcomes. These findings provide additional context for understanding neurological dysfunction as a consequence of viral infection. Critically, these findings also elucidate *resilience* as an outcome to persistent viral infection, provide targets for mechanistic investigations, and expand our understanding of TMEV infection as a model for human neurological diseases.

2. Results

2.1. Expression of Gm41561, a Long Non-Coding RNA Gene, Was Significantly Affected by TMEV Infection Regardless of Mouse Strain

We compared differentially expressed genes between TMEV-infected and sham-infected mice from all CC strains in this study (Supplementary Table S1). Expression of only one gene, *Gm41561*, was significantly different between all infected and uninfected mice, with a log2 fold change value of −17.796. This predicted gene is on mouse chromosome 17 at 31,067,410–31,076,410 base pairs (based on Ensembl annotation of GRCm39), and encodes a long non-coding RNA (lncRNA). Although lncRNAs, including *Gm41561*, tend not to be conserved across species [21], this finding underscores the possibility of similar non-protein-coding loci being commonly involved in human viral infections.

Gm41561 is located approximately 300 kb upstream of the H2 region. This proximity suggests potential linkage between *Gm41561* and H2, which has previously been associated with TMEV susceptibility [6,8,9]. *Gm41561* contained two exons and 815 variant alleles in mice. Any of these variant alleles could have downstream functional consequences; for example, lncRNA splice variants can produce myriad wide-ranging effects as they influence the expression and regulation of multiple genes and their downstream interactants [21]. We found no variants that correlated with the presence or absence of TMEV for any CC strain. However, 949 target genes have been identified as being differentially expressed in adipocytes following knockdown of *Gm41561* [22]. This finding reinforces the likelihood

that *Gm41561* extensively affects gene expression differences in infected vs. sham-infected mice.

Comparing gene expression between pooled infected vs. pooled sham-infected mice was important for determining universal effects of TMEV infection on gene expression, but obscured the effects of the genetic diversity on viral response represented by the 19 CC strains. Therefore, we next compared infected and sham-infected mice from each strain separately, then grouped the strains based on similar phenotype profiles to identify molecular drivers of each profile.

2.2. CC Strains Demonstrated Novel Responses to TMEV Based on TMEV Persistence and Phenotypic Severity

We identified distinct TMEV response profiles by overlaying 90 dpi cumulative phenotype scores, and levels of TMEV RNA measured at 90 dpi (Figure 1). The cumulative phenotype scores are the sum of the scores for multiple phenotypes and therefore represent the totality of TMEV phenotypes over time. These scores were used to compare levels of phenotypic severity experienced by different CC strains.

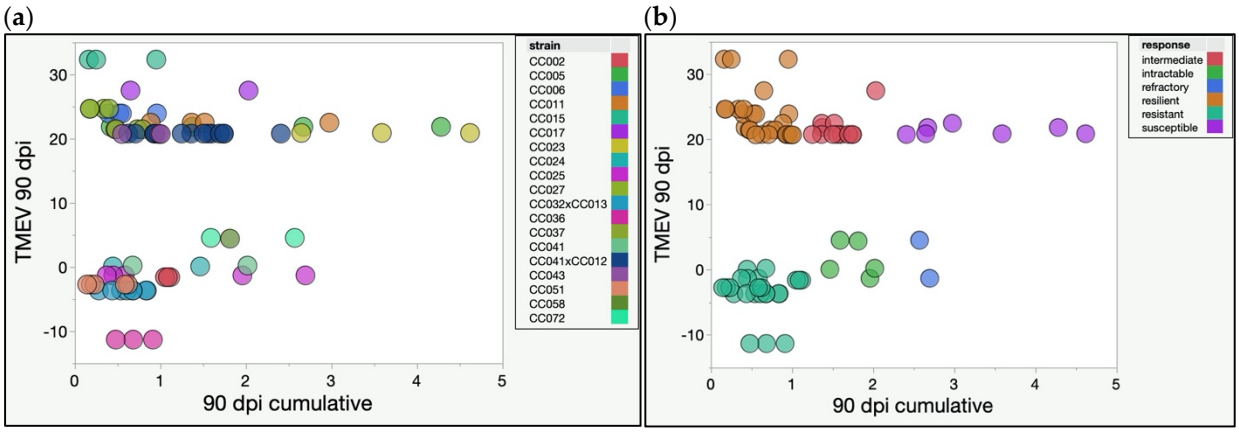

Figure 1. The 90 dpi cumulative scores (cumulative frequencies of hunching, delayed righting reflex, paresis, paralysis, clonus, ruffling, and encephalitis observed over 90 dpi, as described previously [23]) and TMEV RNA levels (shown as log2FoldChange values) at 90 dpi were plotted with different colors for each CC strain (**a**) or response category (**b**).

Infected mice of the same strain had consistent phenotype profiles, demonstrating phenotypic reproducibility. We also found that certain strains consistently clustered together. These clusters represented different TMEV response profiles. Importantly, TMEV persistence, as measured by TMEV RNA levels, did not correlate with phenotype severity, even when considering each of the seven phenotypic classes separately (Figure 2).

Strains with little to no detectable TMEV RNA at 90 dpi had correspondingly low phenotype scores. We termed such strains "resistant" based on the TMEV response described previously for TMEV-"resistant" C57BL/6J mice [20,24]. Resistant strains included CC002, CC032×CC013, CC036, and CC051.

We identified other mouse strains with low cumulative 90 dpi scores, similar to resistant strains, but with high levels of TMEV RNA measured at 90 dpi. The high viral presence and low phenotype scores indicated these strains tolerated the ongoing infection. We called these strains "resilient" because not only did these mice tolerate the virus without succumbing, but they also showed minimal signs of suffering from disease. Resilient strains included CC006, CC015, CC027, CC037, and CC043.

On the other hand, some strains exhibited moderately high cumulative 90 dpi scores, but virtually no TMEV RNA was detected at 90 dpi. We considered these mice to have "intractable" disease, as the cause of the disease symptoms (TMEV) had been effectively eliminated but the symptoms continued to persist. We considered the most severe intractable cases to be "refractory" because cumulative scores in these strains were among

the highest measured, despite low levels of TMEV RNA. Mice of the strain CC072 fell into this category.

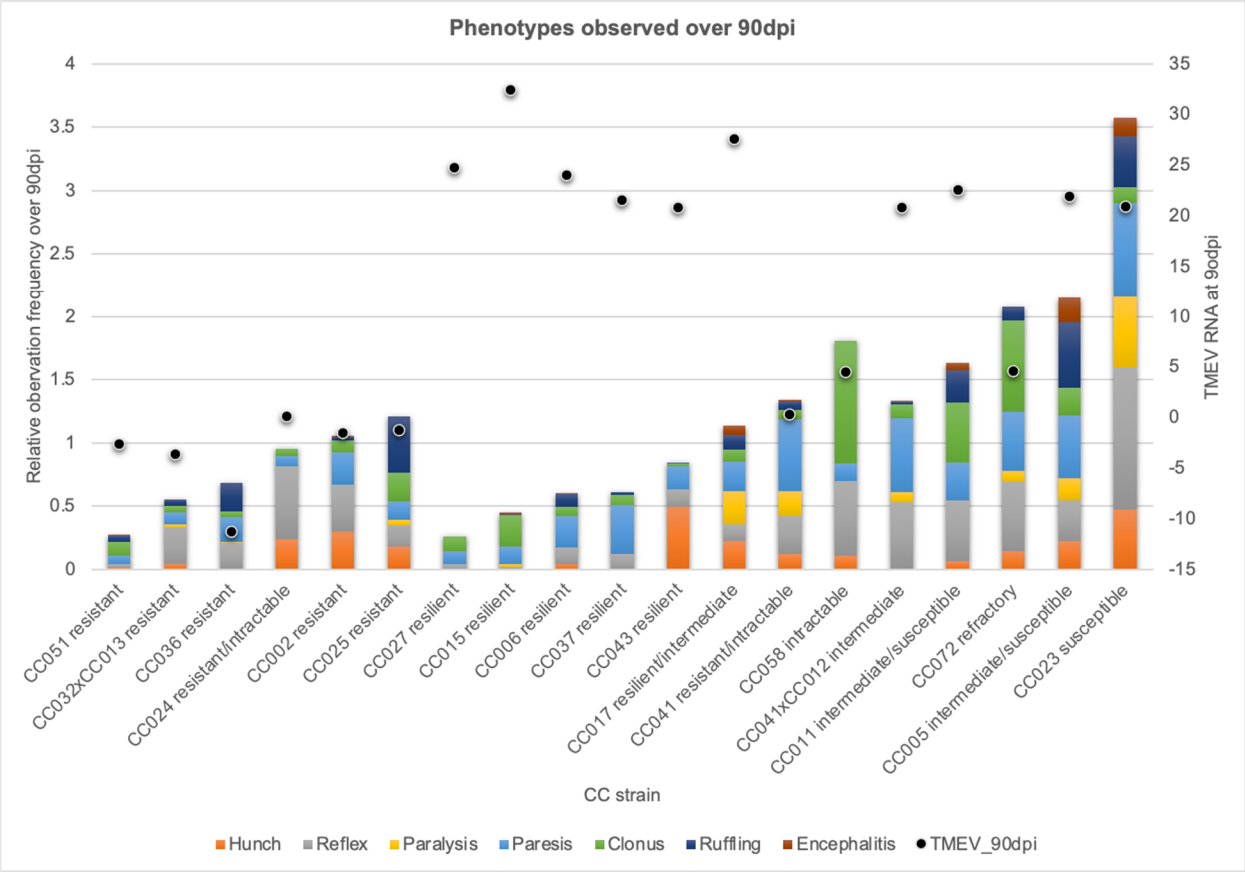

Figure 2. Full 90 dpi cumulative phenotype profiles for each strain are shown with each of the 7 phenotype categories distinguished by color. Strains are ordered from left to right by response category. "Relative observation frequency over 90 dpi" shows the cumulative frequencies of hunching, delayed righting reflex, paresis, paralysis, clonus, ruffling, and encephalitis observed over 90 dpi, as described previously [23]. "TMEV RNA at 90 dpi" shows levels of TMEV RNA measured at 90 dpi (log2FoldChange values) as dots.

Strains with "intermediate" TMEV susceptibility have been described previously [6,25]. Such mice had persistent TMEV infection with moderate cumulative phenotype scores. All but one mouse from strain CC041×CC012 demonstrated an intermediate TMEV response.

Finally, strains with high levels of TMEV RNA and high 90 dpi scores were classified as "susceptible." Susceptible mice in this study included strain CC023. These mice experienced the most severe and debilitating of the TMEV-induced neurological deficits while continuing to show signs of persistent infection.

Mice from other strains included in this study did not fall consistently into a single response category. We could not conclude whether sex played a role in response differences in these strains, due to small numbers of mice per sex/strain combinations. However, individual mice within each of these strains exhibited similar TMEV responses. We therefore classified these strains as follows: CC005 and CC011—intermediate/susceptible; CC017—resilient/intermediate; CC024 females—intractable, CC024 males—resistant; CC025—all but one mouse scored as resistant; CC041 females—resistant, CC041 males—intractable; CC058—intractable.

2.3. Genetic Diversity Contributed to Protection, Compensation, or Capitulation in the Face of TMEV Infection

We used Ingenuity Pathways Analysis to better understand the overall influence of TMEV infection (Table 1). This analysis included all statistically significant DEGs for all strains. Two top Canonical Pathways were identified: Neuroinflammation Signaling Pathway and GABA Receptor Signaling. Each pathway has been implicated in neurodegenerative diseases (e.g., [26]) and viral infections (e.g., [27]).

Table 1. Top 5 canonical pathways for categories described in this study, along with their respective *p*-values [28], and the key molecules (genes or complexes) involved in these pathways. Arrows indicate the direction of gene expression (increased or decreased) in infected versus uninfected mice, based on the averaged expression values for strains included in each response. Additional information for these molecules, including descriptions and strain-specific expression, is available in Supplementary Table S1.

Top 5 Canonical Pathways	*p*-Value	Molecules
Overall		
Neuroinflammation Signaling Pathway	1.32×10^{-2}	GABRA6 ↓
GABA Receptor Signaling	2.94×10^{-2}	GABRA6 ↓
Resistant		
Neuroprotective Role of THOP1 in Alzheimer's Disease	2.59×10^{-3}	HLA-A ↑, PRSS41 ↑
The Visual Cycle	1.29×10^{-2}	RDH13 ↑
Retinoate Biosynthesis I	2.31×10^{-2}	RDH13 ↑
Antigen Presentation Pathway	2.50×10^{-2}	HLA-A ↑
B Cell Development	2.75×10^{-2}	HLA-A ↑
Resilient		
Primary Immunodeficiency Signaling	8.23×10^{-4}	CD4 ↑, Igha ↑, IGHG1 ↑, Ighg2b ↑
IL-7 Signaling Pathway	3.21×10^{-3}	Igha ↑, IGHG1 ↑, Ighg2b ↑, Ighg2c ↑
Role of Pattern Recognition Receptors in Recognition of Bacteria and Viruses	7.53×10^{-3}	IFIH1 ↑, IL25 ↑, LTA ↑, Oas1b ↑, Oas1d ↓ (includes others)
Phagosome Maturation	8.14×10^{-3}	DYNLT1 ↑, HLA-A ↑, HLA-E ↑, PRDX1 ↑, TUBD1 ↑
Th1 and Th2 Activation Pathway	1.12×10^{-2}	Aph1c ↓, CD4 ↑, HLA-A ↑, IL25 ↑, LTA ↑
Susceptible		
NRF2-mediated Oxidative Stress Response	5.01×10^{-3}	AOX1 ↑, PPIB ↑
Role of JAK2 in Hormone-like Cytokine Signaling	1.92×10^{-2}	PRL ↓
Nicotine Degradation III	3.20×10^{-2}	AOX1 ↑
Activation of IRF by Cytosolic Pattern Recognition Receptors	3.53×10^{-2}	PPIB ↑
Nicotine Degradation II	3.64×10^{-2}	AOX1 ↑

We next tested the hypothesis that different TMEV response profiles were associated with distinct gene expression profiles. For this, we developed gene expression profiles for each strain using the Analyses feature of IPA. We then used the Comparison Analysis feature of IPA to compare CC strains within each TMEV response category and identify similarly affected networks, biological functions, and canonical pathways.

Canonical Pathways analyses included statistically significant DEGs for strains of the resistant, resilient, and susceptible TMEV response categories. Top Canonical Pathways varied by response group, with some pathways shared between groups as well (Figure 3). The pathway "Activation of IRF by cytosolic pattern recognition receptors" was significantly affected across all groups, suggesting that all mice recognized the presence of the virus, irrespective of their different responses. For resistant strains the most significant Canonical Pathway was "Neuroprotective Role of THOP1 [Thimet oligopeptidase] in Alzheimer's Disease" ($-\log p = 2.59$). This same pathway was also significant, though to a lesser degree, for resilient ($-\log p = 1.87$) and susceptible ($-\log p = 1.19$) strains. In fact, no significant canonical pathways were unique to the resistant response profile. This

indicates "resistance" was based on the relative degree to which certain pathways (or the genes involved) were affected.

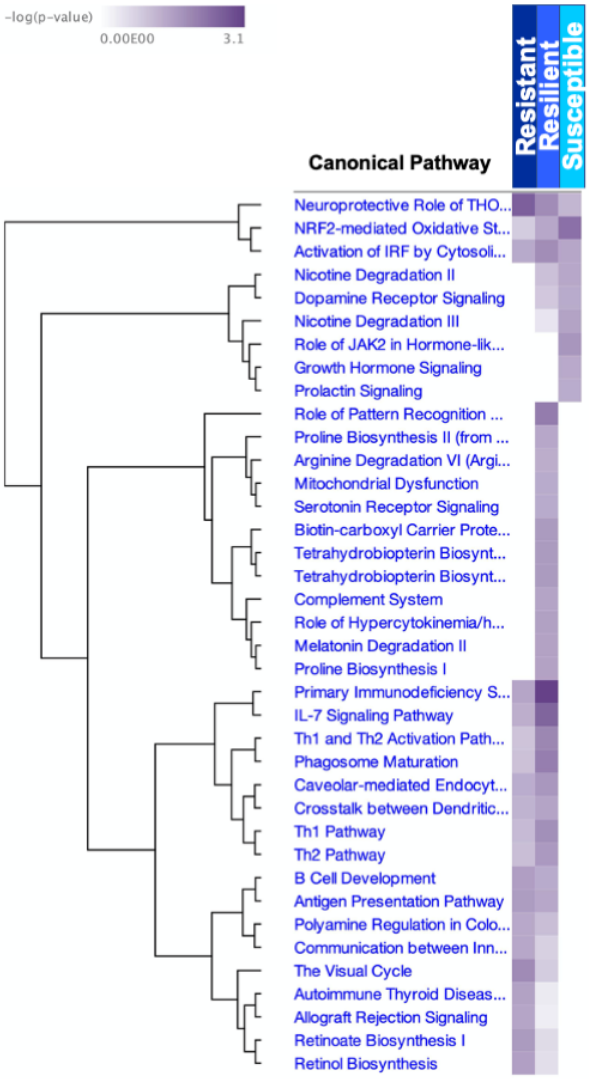

Figure 3. Significant Canonical Pathways are listed for each response group. The significance of each pathway to each response group is shown as –log (*p*-value), with darker shading indicating greater significance.

The top Canonical Pathway for resilient strains was "Primary Immunodeficiency Signaling" ($-\log p = 3.08$), which was also significant in resistant strains ($-\log p = 1.46$) but not susceptible strains. Additionally, 12 Canonical Pathways were significant only for resilient strains. The most significant of these was "Role of Pattern Recognition Receptors in Recognition of Bacteria and Viruses" ($-\log p = 2.12$).

"NRF2-mediated Oxidative Stress Response" was the top Canonical Pathway for the susceptible category ($-\log p = 2.30$). This pathway was also significant in resilient ($-\log p = 1.42$) strains, though to a lesser extent. Three significant pathways were unique to the susceptible response category: "Role of JAK2 in Hormone-like Cytokine Signaling" ($-\log p = 1.72$), "Growth Hormone Signaling" ($-\log p = 1.40$), and "Prolactin Signaling" ($-\log p = 1.34$). The same molecule, prolactin (PRL), was involved in all three of these pathways. PRL was not involved in pathways related to resistant or resilient responses.

We next performed gene network analyses to identify networks connecting gene expression differences with biological functions and diseases. These analyses demonstrated

how the roles of specific molecules were influenced by overall host genetic background. We identified top networks for all strains together ("overall"), and for resistant, resilient, and susceptible strains separately (Supplementary Table S2). We then investigated the diseases and biological functions that could be expected to be significantly affected by TMEV infection, based on genes in top networks (Supplementary Table S3), using the IPA "Downstream Effects Analysis."

Networks for the overall group all had scores of three, indicating these networks had low chances of potential causal relevance (for more details about IPA scoring, refer to [29]). Nevertheless, the molecules in those networks had functions known to be perturbed in other viral infections of the CNS. For example, TBX19 is involved in the accumulation of progenitor cells; reduced proliferation of neural stem/progenitor cells and impaired adult neurogenesis have also been observed in herpes simplex 1 infection [30]. Another function of TBX19 potentially affected by TMEV infection was "Development of pituitary gland;" pituitary dysfunction following acute viral meningoencephalitis (e.g., [31,32], reviewed in [33]) and viral meningitis (e.g., [34]) have been reported. Despite the low network scores, evidence suggested that TMEV-induced perturbations in gene expression could affect developmental and endocrinological biological functions, along with immune and neurological functions.

Next, we identified the networks and diseases/biological functions affected by TMEV for each response group. The top network for resistant strains (score of 27) is related to biological functions generally involving repair and regulating cytotoxic immune responses. Many top networks were listed for resilient strains, the highest with a score of 41; many functions associated with these networks pertain to inflammation and innate immune response as well as development and cell cycle regulation. For the susceptible category, functions related to the single network (score of 46) involve hormone-sensitive responses and regulation which collectively affect cell signaling and cell cycle. Among biological functions affected by these networks, "Small Molecule Biochemistry" was the only one shared by all categories. However, this function is listed in different contexts for different categories: for resistant strains, the same network that affects "Small Molecule Biochemistry" also affects "Energy Production" and "Lipid Metabolism." In resilient strains, the same network affecting "Small Molecule Biochemistry" also affects "Cell-To-Cell Signaling and Interaction" and "Humoral Immune Response;" for susceptible strains, "Cell Signaling" and "Cell Cycle" are affected by the same network as "Small Molecule Biochemistry." Only one gene, peptidylprolyl isomerase B (*Ppib*), was listed for resistant, resilient, and susceptible TMEV response groups under the category "Small Molecule Biochemistry" (Supplementary Table S3); in each case, the role of *Ppib* was related to cytotoxicity.

To identify common effects of TMEV infection that manifested differently depending on context, we characterized the molecules in each network (including genes and complexes) which effected biological functions across multiple response groups. We noted 37 molecules found in >1 networks. Of these molecules, 15 were found in networks for both resistant and resilient strains, 13 for resilient and susceptible, 2 for resistant and susceptible, and 5 were included in networks for all three response groups. Additionally, one gene (*Igkv4-61*) was found in networks for susceptible and overall, and one complex (MHC class II) in networks for resilient, susceptible, and overall. In resilient strains, three networks included the Il-12 complex. These findings reflect the multiple roles played by each gene/complex, roles which vary based on the broader "expression context" of a given TMEV response category.

2.4. Upstream Regulators of Biological Functions and Their Molecular Targets, Varied by TMEV Response Group

For each of the different TMEV response groups, we identified the top five Upstream Regulators (URs), specific genes with expression connected to the biological functional categories influenced by the networks/molecules in Supplementary Tables S2 and S3 (Table 2). Most (four out of five) of the URs associated with the "Overall" group regulate transcription; the UR miR-122-5p is a microRNA known to regulate antiviral responses

in humans, particularly in hepatitis C infection (e.g., [35,36]). The target of regulator NFIA (nuclear factor I A), GABRA6 (gamma-aminobutyric acid receptor subunit alpha-6), interacts with the inhibitory neurotransmitter GABA.

Table 2. Top 5 upstream regulators for each category described in this study, along with their respective *p*-values and target molecules (genes and complexes). Here, "*p*-value of overlap" indicates the significance of overlap between genes of this dataset and those influenced by the upstream regulator, using Fisher's exact *t*-test [37]. Arrows indicate the direction of gene expression (increased or decreased) in infected versus uninfected mice, based on the averaged expression values for strains included in each response. Additional information for these regulators and molecules, including descriptions and chromosomal locations, is found in Supplementary Table S1.

Top 5 Upstream Regulators	*p*-Value of Overlap	Target Molecules
Overall (Infected vs. Sham)		
NFIA ↑	1.37×10^{-3}	GABRA6 ↓
miR-122-5p (miRNAs w/seed GGAGUGU)	4.42×10^{-3}	TBX19 ↓
TAF7L ↓	5.16×10^{-3}	TBX19 ↓
EP300 ↓	2.39×10^{-2}	TBX19 ↓
GATA2 ↑	2.69×10^{-2}	TBX19 ↓
Resistant		
MSH2 ↑	1.30×10^{-5}	IGHG1 ↑, IGKC ↑
IL21R ↑	7.54×10^{-5}	IGHG1 ↑, IGKC ↑
CXCL10 ↑	1.77×10^{-4}	*Ccl6* ↓, IGKC ↑
HSP-990	6.24×10^{-4}	HLA-A ↑
Raet1d ↑/Raet1e ↑	6.24×10^{-4}	HLA-A ↑
Resilient		
MSH2 ↑	4.33×10^{-5}	IGHG1 ↑, Ighg2b ↑, IGKC ↑
PNPT1 ↑	5.38×10^{-5}	*Apol9a* ↑/*Apol9b* ↑, GBP6 ↑, IFI16 ↑, IFIH1 ↑, *Oas1b* ↑
Irgm1 ↑	1.54×10^{-4}	*Apol9a* ↑/*Apol9b* ↑, GBP6 ↑, IFI16 ↑, IFIH1 ↑, *Oas1b* ↑, *Oas1d*↓ (includes others)
IFNB1 ↑	1.63×10^{-4}	GBP3 ↑, GBP6 ↑, GLP2R ↑, HLA-A ↑, IFI16 ↑, IFIH1 ↑, MCM10 ↑, *Oas1b* ↑, *Oas1d* ↓ (includes others), TRIM6-TRIM34 ↑
ELAVL1 ↓	3.09×10^{-4}	CASP9 ↓, GBP6 ↑, HLA-A ↑, IFI16 ↑, IFIH1 ↑, *Igha* ↑, *Igkv8-30* ↑, *Oas1b* ↑
Susceptible		
GNAS ↑	5.07×10^{-4}	GDF9 ↓, PRL ↓
BIM 23A760	5.82×10^{-4}	PRL ↓
IQUB ↑	5.82×10^{-4}	PRL ↓
RHOQ ↓	5.82×10^{-4}	PRL ↓
UBE2Q1 ↑	5.82×10^{-4}	PRL ↓

The Resistant and Resilient groups shared only one UR in common (MSH2, mutS homolog 2), but the molecules targeted by the URs of these two groups overlapped somewhat. Only one target molecule differed in the Resistant group compared to Resilient: *Ccl6* (chemokine [C-C motif] ligand 6), a type of small cytokine only found in rodents. Other URs for the Resistant group had well-known, multifaceted roles in controlling the immune response. For example, C-X-C motif chemokine ligand 10 (CXCL10) also stimulates multiple types of immune cells and has known roles in neuronal injury related to viral infection and in relevant human disorders such as multiple sclerosis [38]. Retinoic acid early transcripts 1D/1E (*Raet1d*/*Raet1e*), related to major histocompatibility complex class I genes, are part of a family of glycoproteins involved in immune responses and expressed in pathological conditions, notably experimental autoimmune encephalomyelitis in mice [39] and mouse cytomegalovirus [40]. The "outlier" of the URs for the Resistant group was heat shock protein 990 (HSP-990), a synthetic HSP90 inhibitor with potential therapeutic use in

cancer treatment [41]. Hsp90 has been identified as an important host factor in the life cycle of TMEV [42]: Hsp90 colocalizes with the VP1 subunit of TMEV during infection [43].

URs for the Resilient group, aside from MSH2, included polynucleotide phosphorylase (PNPT1), an enzyme which has been associated with a spectrum of neurodegenerative phenotypes (e.g., [44,45]). Another UR encodes immunity-related GTPase family M protein 1 (*Irgm1*), which modulates resistance to pathogens [46,47] and can contribute to autoimmunity [48,49]; similarly, the UR interferon beta 1 (IFNB1) is crucial for the antiviral immune response but can also contribute to autoimmunity (reviewed in [50,51]). Finally, the UR ELAV-like RNA binding protein 1 (ELAVL1) functions in regulating the innate immune response via its RNA binding capabilities [52,53]. Together, these URs targeted many more molecules in addition to those listed for the Resistant group. The functions of these UR target molecules gave some insight into the molecular differences distinguishing the responses of the resilient strains. Other targets contributing to the antiviral response included interferon gamma inducible protein 16 (IFI16), which mediates interferon beta production in response to viral infection [54], and interferon induced with helicase C domain 1 (IFIH1), which senses viral RNA to provoke an antiviral immune response and occasionally contributes to autoimmune diseases (for example, [55]). The protein encoded by the target gene 2′–5′ oligoadenylate synthetase 1B (*Oas1b*) was found to affect susceptibility to West Nile Virus in CC mice [56]. The target molecules *Apol9a/Apol9b* function to inhibit TMEV replication [57]. Variants of target molecules GBP3 and GBP6 (guanylate binding proteins 3 and 6) have antiviral activity (e.g., [58]).

Susceptible group URs included guanine nucleotide-binding protein, alpha subunit (GNAS), an imprinted (i.e., methylation-regulated) locus with a complex expression pattern. GNAS is implicated in the production and function of hormones that regulate endocrine glands, such as the pituitary gland and thyroid, along with ovaries and testis. Another UR identified was the compound BIM-23A760, a chimeric somatostatin/dopamine agent used for controlling proliferation of non-functioning pituitary adenomas [59–61]. The IQ motif and ubiquitin domain-containing protein may contribute to cell proliferation and migration by activating the Akt/GSK3β/β-catenin signaling pathway [62]. The UR Ras homolog family member Q (RHOQ) has an important function in nerve regeneration/elongation [63,64] and a role in physiological B cell responses [65]. Finally, the UR ubiquitin conjugating enzyme E2 Q1 (UBE2Q1) is regulated via methylation and functions to flag proteins for degradation by modifying them with ubiquitin [66]. UBE2Q1 is a potential biomarker for hepatocellular carcinoma [67–69] and ovarian cancer [70], and may also function in female hormone homeostasis (for example, [71]). All five top URs for the susceptible group target prolactin (PRL); GNAS also targets growth differentiation factor 9 (GDF9). GDF9 regulates ovarian function [72,73]. PRL, meanwhile, is also a growth regulator, including for the immune system (for example, [74,75]).

2.5. Unique Biomarkers Distinguished TMEV Response Categories

We identified known and novel molecular biomarker candidates for each CC strain using the Biomarker Filter Results feature of IPA, filtering by species (mouse), tissues (nervous system), and *p*-adj value equal or less than 0.05 (except for the overall group, where the average *p*-adj value was 0.999). We then used the Biomarker Comparison Analyses feature to compare biomarker differences and similarities across different TMEV response profiles, and to identify unique biomarkers for each (Table 3).

For the overall group, we performed a Biomarker Filter Analysis to identify potential biomarkers which could reveal common molecular contributors to TMEV's overall effects across multiple genetically diverse strains. One biomarker resulted from this analysis: staufen double-stranded RNA binding protein 1 (STAU1). STAU1 has been found to promote viral replication in several types of viral infections (for example: influenza [76], human immunodeficiency virus type 1 [HIV-1, [77]], human endogenous retrovirus [HERV-K, [78]], and Ebola [79]). Expression levels for *Stau1* were all low in infected vs. sham-infected mice, and varied little across all strains in this study (Supplementary Table S1).

Table 3. Unique biomarkers representing 3 distinct TMEV response profiles were identified from expression data of strains in each category.

Symbol	Entrez Gene Name	Expr Log Ratio	Expr *p*-Value
	Overall		
STAU1	staufen double-stranded RNA binding protein 1	−0.002	0.999
	Resistant		
HLA-A	major histocompatibility complex, class I, A	10.265	1.92×10^{-2}
	Resilient		
CDPF1	cysteine rich DPF motif domain-containing 1	−1.384	1.62×10^{-3}
FGF4	fibroblast growth factor 4	−16.685	3.07×10^{-4}
	Susceptible		
EIF3J	eukaryotic translation initiation factor 3 subunit J	−6.53	8.03×10^{-3}
GDF9	growth differentiation factor 9	−3.6	3.57×10^{-2}
Gm5148/Rps23rg1	ribosomal protein S23, retrogene 1	−8.529	4.00×10^{-2}
MID1	midline 1	−5.28	8.03×10^{-3}
PRL	Prolactin	−17.432	6.52×10^{-3}

The sole biomarker for the resistant group, HLA-A, appeared in the top-scoring networks of both resistant and resilient groups (Supplementary Table S2). However, it was listed as a molecule relevant to diseases and biological functions far more often for the Resistant group (32 vs. 8; Supplementary Table S3). HLA-A is not a mouse gene; rather, this class I gene in the major histocompatibility complex of humans is homologous to several class I genes in mice (*H2-D1*, *-K1*, *-Bl*, *-Q1*, *-Q2*, *-Q4*, *-Q6*, and *-Q10*).

The two biomarkers for the resilient group, *Cdpf1* and *Fgf4*, offered insight into what distinguished the resilient strains from other TMEV responses. The biological functions with which these biomarkers were associated included cancers (i.e., cell growth, transformation, and survival), cell signaling (including binding and adhesion of blood cells and myelosuppression, all likely related to inflammation), and infectious diseases (binding of viruses). Other related functions included tissue morphology, molecular transport, and protein phosphorylation.

Gene expression levels (Table 3, Expr Log Ratio column) for biomarkers of the susceptible response were markedly lower than for any other strain. Biomarker EIF3J (*Eif3j2* in mice) had roles in protein synthesis, metabolism, and translation, sharing these networks with another biomarker, *Mid1*. *Mid1* was associated with nervous system development in the susceptible category, but for resilient strains *Mid1* was more often found in networks related to innate immune response and inflammation. *Gm5148* was represented in only one network, with the biofunction "phosphorylation of protein," listed with the resilient category despite *Gm5148* being a biomarker for susceptible response. *Gm5148* was listed with *Rps23rg1*, a mouse gene on a different chromosome and having different functions altogether; however, *Rps23rg1* was not included in any networks for any groups.

The two remaining biomarkers, *Gdf9* and *Prl*, were found only in networks listed for the susceptible response category. Their biological functions in this context were primarily endocrine-related.

2.6. Haplotypes Provided Context for Pleiotropy and Predictive Alleles

Founder haplotypes (alleles) were identified for 89 genes that effected biological functions relevant to TMEV responses, including genes present in multiple networks, genes present in canonical pathways, URs, UR target molecules, and biomarkers (Supplementary Table S4). Increased heterozygosity of these genes was often associated with resistant or resilient TMEV responses: 13 out of 89 genes were heterozygous in two (out of four) resistant strains, and one gene (*Sfi1*) was heterozygous in three resistant strains. Five genes were also heterozygous in two (out of five) resilient strains. In the susceptible category, only two genes were heterozygous. Of particular interest was the HLA-A region,

due to its historical context with TMEV infection: resistant strains CC032×CC013 and CC015, and resilient strains CC006 and CC027, were heterozygous for the HLA-A region.

Strains from resistant, resilient, and susceptible groups shared the same homozygous founder haplotype for nine genes (Supplementary Table S4). However, it was more common for strains of the same response group to share haplotypes with one another than with strains of other response groups. For example, in the four strains of the resistant group, seven out of the eight possible alleles for *Tmem203* were inherited from the founder strain 129S1/SvImJ; the 129S1/SvImJ haplotype was not found in resilient or susceptible strains. For the gene *Nnmt*, eight of ten founder alleles for the resilient group were inherited from the founder strain WSB/EiJ; the WSB/EiJ haplotype was not present in other strains. For resistant mice, the majority of alleles for six genes were inherited from a founder strain not represented in the alleles for resilient and susceptible mice. Similarly, the predominant alleles of eight genes were found only in resilient strains. The susceptible strain CC023 shared the fewest haplotypes with other strains and groups: there were 21 genes with CC023-specific founder alleles. One surprising exception was the HLA-A region, for which resistant strain CC002 and susceptible strain CC023 shared the same haplotype, inherited from 129S1/SvImJ.

To determine the possible functional relevance of response group-specific haplotypes, we identified sequence variants inherited from each founder strain for those genes with the highest response-specific allele frequencies: *Tmem203* for resistant strains, and *Nnmt* for resilient strains. We found no SNPs or sequence variants unique to the 129S1/SvImJ founder strain from which most resistant mice inherited *Tmem203*. However, we identified SNPs and sequence variants for *Nnmt* that were unique to WSB/EiJ, the most common founder allele for this gene in resilient strains. Two of these variants were classified as transcription factor-binding site variants (SNPs rs263473586 and rs1132394264), located 8bp from each other upstream of *Nnmt*. Both of these variants were located within a CTCF binding site (ENSMUSR00000747534) associated with regulatory action in the developing mouse brain. In our search for *Nnmt* variants we also uncovered 19 additional SNPs and two indels, which were identified as upstream gene variants associated with miRNA ENSMUSG00002076361. We next identified a *Nnmt* sequence variation specific to the A/J founder strain, relevant to susceptible strain CC023 (and intermediate/susceptible strain CC011). The only unique and potentially functionally relevant sequence variation identified for the A/J strain was SNP rs1134607613, an upstream gene variant associated with miRNA ENSMUSG00002076361, and located farther upstream than the WSB/EiJ variants. We did not measure miRNA expression in this study and therefore could not evaluate how these variants influenced expression of ENSMUSG00002076361. However, because all these variants were upstream of the pairing region of the miRNA, it is reasonable to expect these variants could affect its production [80,81]. ENSMUSG00002076361 was not listed in miRBase [82], but a sequence comparison (blastn) of its sequence revealed similar sequences present on at least 11 other chromosomes. MiRNAs can have pleiotropic effects in that they can regulate multiple genes [80]. Therefore, these similar sequences could reflect targets of this miRNA.

3. Discussion

In this study using genetically diverse mouse strains, we evaluated interactions between DEGs and how these interactions contributed to different long-term outcomes to TMEV infection. By comparing gene expression profiles in TMEV-infected and control mice of the same strain, we reduced the background "noise" and focused only on the effects of TMEV infection in each strain. The TMEV response profiles produced with this approach allowed us to associate significant DEGs with TMEV response (phenotype severity). In doing so, we identified a novel response, "resilience," characterized by relatively mild symptom profiles with high levels of TMEV RNA. This contrasts with the current paradigm of TMEV infection, wherein strains considered "susceptible" to persistent TMEV infection develop demyelinating disease and "resistant" strains clear the infection and experience

seizures. While such clear-cut distinctions are helpful for, e.g., mechanistic studies of demyelination, human outcomes to viral infection tend to be far more nuanced.

Comparisons of DEGs among individual strains, even between TMEV response groups, revealed few strong correlations between gene expression and TMEV outcome. For most of the 89 genes that were the focus of this study, expression levels differed little among strains (Supplementary Table S1). We found it more appropriate to generate response-specific expression profiles, placing individual genes in context of pathways and networks.

As expected, we found resistant mouse strains showed evidence of an appropriate and effective immune response mediated by the major histocompatibility complex class I region. The top Canonical Pathway for resistant strains, "Neuroprotective role of THOP1 in Alzheimer's Disease," is associated with enhanced protection against neurodegeneration [83,84] and enrichment of this pathway in the resistant strains may explain the mild neurological symptoms observed in these mice. The sole biomarker for the resistant group, HLA-A, has a critical role in the immune system and, by extension, responses to infectious agents such as viruses. Expression levels of the mouse homologs of HLA-A did not correlate directly with TMEV response; however, the mouse HLA-A homologs have thousands of polymorphic alleles—sequence variants with cumulative effects on immune response. The role of H2 class I alleles in TMEV infection has been described for inbred mouse strains [6,8,9] and for the CC strains included in this study [23,85]. Though the H2 class I region was inherited from the same founder strains for some CC strains of different response categories, interactions between the HLA-A homologs and other genes within the same networks influenced the TMEV-resistant outcome.

Resilient strains failed to eliminate the viral infection but moderated its effects, possibly by disabling the virus or reducing its virulence, for example by inhibiting TMEV replication or enhancing RNA degradation. Members of the top Canonical Pathway for resilient strains, "Primary Immunodeficiency Signaling," can provide protection against immune depletion while inhibiting viral spreading. Differential expression of pathway molecules may therefore serve in a compensatory fashion for the resilient strains as these mice maintain a relatively heavy viral load while experiencing minimal symptoms. However, primary immunodeficiency often coincides with/causes autoimmunity [86–90]. This seemingly paradoxical co-occurrence—a deficient immune response coupled with a powerful immune response—results from complex interactions between different signaling pathways, and is the product of hereditary factors [87]. While a deficient immune response could help explain the relatively high levels of TMEV RNA measured in resilient strains at 90 dpi, other pathways collaborated to ensure these mice continued to live relatively symptom-free lives. Among the pathways significant only for resilient strains, the most significant was "Role of Pattern Recognition Receptors in Recognition of Bacteria and Viruses." Different classes of germline-encoded pattern recognition receptors can recognize pathogens and trigger innate and adaptive immune responses (reviewed in [91,92]). Genetic differences contribute to the relative effectiveness of innate immune responses to TMEV infection, as described for resistant and susceptible inbred strains (e.g., [93,94]). Different substrains of BALB/c mice exhibit varying levels of susceptibility to TMEV-induced demyelination, including an "intermediate" response [95], so there is precedent for a response to TMEV that is neither resistant nor susceptible; however, to our knowledge the current study is the first to characterize a resilient response to TMEV infection. The resilient strains may be able to control the virus to a level whereby it could no longer cause damage, but may still persist. Though resilient strains retained TMEV RNA into the late chronic phase of infection, these mice survived and maintained biological functions, implicating crucial roles for non-immune networks and molecules. Resilient strain networks included categories of molecules containing both biomarkers *Cdpf1* and *Fgf4* with HLA-A. These categories/molecules were associated with cancers and with organismal injury and abnormalities (Supplementary Table S2). Further, the resilient group biomarker FGF4 promotes stemness and proliferation of human stem cells [96,97]. Taken together, our

findings suggest a balanced relationship between cell growth and survival, and immune response/recognition, in the resilient strains.

The most susceptible group was characterized by a relative paucity of immune-related pathways and regulators. Instead, the response of the susceptible mice appears to have been hampered by endocrine-related factors. The susceptible strain biomarkers indicated the environment in which these mice failed to thrive in the face of TMEV infection. *Rps23rg1* has been associated with reduced beta-amyloid levels in Alzheimer's disease [98,99]; deletion of this gene decreases synaptic integrity and function [100]. Next, *Mid1* is normally strongly upregulated in murine cytotoxic lymphocytes and plays a role in granule exocytosis [101]. In humans infected with rhinovirus, Mid1 is normally upregulated in bronchial epithelial cells, suggesting a link to innate immune pathway activation and inflammation [102]. Finally, the *Prl* gene has multiple roles relevant to TMEV outcomes: *Prl* can stimulate cells of adaptive and innate immune responses [103], is neuroprotective, and has promyelinating properties [104–106]. Therefore, prolactin could have a beneficial effect on the neurological and immunological outcomes of TMEV infection. However, *Prl* expression levels were very significantly decreased for infected susceptible mice compared to uninfected mice (fold change −17.432). The top URs for the susceptible group all decreased prolactin gene expression. This may indicate a response meant to counter another, harmful effect of prolactin: inflammation that leads to autoimmunity [107–112]. Further mechanistic studies are needed to better understand the roles of *Prl* in relation to TMEV infection and neuropathology.

Haplotype and allelic variation demonstrated how the genetic diversity of the CC strains contributed to the phenotypic diversity underlying the different TMEV response groups. We identified sequence variants with potential functional relevancy by identifying genes (from the list of 89 genes of interest) for which a single founder strain was the most common source of alleles for strains of a specific TMEV response group. We have in this way identified potential targets for future mechanistic studies. In particular, the strong association of *Nnmt* haplotypes with the resilient TMEV response group suggested a potential role for this gene in resilience.

In the present study, we compared sequence variation across the CC founder strains with a focus on those variants specific to the WSB/EiJ founder (associated with the resilient response group for *Nnmt*) and A/J founder (associated with the susceptible group for *Nnmt*). *Nnmt* has been associated with neurodegeneration and Parkinsonian behavior in humans [113,114] and the model organism *C. elegans* [115], and more recently with Alzheimer's disease [116]. Dysregulation of *Nnmt* is recognized as a contributor to neurological diseases, cancers, and obesity (e.g., [116–120]). In fact, at least one *Nnmt* sequence variant has been connected with neurological disease in humans [119]. Interestingly, *Nnmt* has also been shown to have neuroprotective effects [121]. Most of the resilience-associated SNPs and indels we identified within the *Nnmt* gene were synonymous SNPs unlikely to contribute to functional differences. Two variants, however, were associated with a regulatory element: a CTCF binding site. The CTCF zinc finger protein has myriad genetic and epigenetic regulatory capabilities, and plays numerous functional roles via its capacity for context-dependent ("custom") gene regulation [122–125]. We did not find any *Nnmt* sequence variants with functional relevance for the susceptible response.

Our search for sequence variation relevant to *Nnmt* also uncovered variants associated with a miRNA gene located in close proximity to *Nnmt*. Resilient strains contained 19 such variants; susceptible mice had one variant. These miRNA-associated variants could influence the production of the miRNA and, by extension, its regulatory capacity [126]. The regulatory function of miRNAs results in pleiotropy: basically, a single gene influencing the expression of many other genes [80]. SNPs affecting miRNAs are implicated in neurological conditions (reviewed in [127–129]), and many other complex diseases [130]. Furthermore, recent studies describe miRNA links between Epstein–Barr virus and multiple sclerosis [131–133], adding plausibility to the idea of miRNA involvement in TMEV response.

In fact, miR-219 has been associated with reduced TMEV replication and TMEV-induced demyelination [134], though TMEV itself does not appear to be a target of miRNAs [135].

Taken together, our findings suggest that variations specific to the genetic background of the host interact with the rest of the genome in a "domino effect" resulting in different categories of TMEV response. While one path of this "domino effect" leads to TMEV clearance or persistence, the next path can lead to symptoms that persist or worsen (susceptibility) or improve or even appear to resolve entirely (resilience). Smaller "branches" off these different paths lead to minor nuances in TMEV outcome, such as TMEV-induced symptoms that remain intractable even once the virus is cleared. The larger pathways and networks involved in the broader TMEV outcomes (resistant, resilient, and susceptible) provide targets for future studies to reveal the mechanisms underlying different responses to TMEV.

4. Materials and Methods

4.1. Mice and Phenotyping

Ethics statement: All procedures were approved by the Institutional Animal Care and Use Committee at Texas A&M University and performed under animal use protocol numbers 2017-0082 (approved 20 July, 2017) and 2020-0065 (approved 21 May, 2020). All experiments were performed in accordance with relevant guidelines and regulations. Mice were group-housed and all testing performed during the light phase.

As described in [23], at 4 weeks of age, female and male mice were anesthetized by isoflurane inhalation (MWI, Meridian, ID, USA) and injected intracerebrally with 5.0×10^4 plaque-forming units (PFU) of the BeAn strain of TMEV (American Type Culture Collection [ATCC] VR 995, Manassas, VA, USA) in 20 µL of PBS placed into the fenestra at a depth of approximately 1.5 mm [136,137]. Sham-infected mice (n = 25 females and 27 males) were anesthetized and injected with PBS only. We used the "cumulative phenotype score (90 dpi score)" as defined in [23] to quantitatively compare TMEV outcomes across strains. Briefly, multiple phenotype classes were scored daily during the acute phase of infection (0–14dpi) and weekly thereafter (15–90 dpi). These classes included hunching, righting reflex, paralysis, paresis (weakness), clonus, ruffling (piloerection), and encephalitis, detailed in [23]. The sum of the scores for these phenotypes was the "cumulative phenotype score," called "90 dpi score," as the value reflects the frequency of observation for multiple neurological phenotypes over 90 dpi.

Numbers of mice of each sex and infection status for each strain, along with the average TMEV RNA levels measured at 90 dpi, and average cumulative scores at 90 dpi, are shown in Table 4. Whenever possible, littermates were used to avoid batch effects within a strain.

4.2. RNA Isolation and Sequencing

RNA was isolated from hippocampi and thoracic spinal cords of 145 mice of 19 CC mouse strains (see Table 1 for details) and quantified with the Qubit Fluorometer (Life Technologies, Carlsbad, CA, USA) with a broad range RNA assay. Concentrations were normalized for library preparation, and RNA quality was verified on the Agilent TapeStation with RNA ScreenTape. RNA of sufficient quantity and quality was not uniformly available for infected and uninfected mice of both sexes for all strains; therefore, RNA sequencing data reflect a mixture of the two tissues. While not ideal for understanding tissue-specific gene expression, this procedure nonetheless allowed an overview of gene expression changes related to TMEV infection. Details regarding the generation of RNA sequencing libraries and sequencing procedures, including downstream processing and quality control, have been reported previously [23]. To evaluate the relative persistence of TMEV at 90 dpi, we measured expression (Fold Change) of the polyprotein AAA47930.1 of the TMEV virus after DEG (Differentially Expressed Genes) test was calculated using DESeq2 based on infection state (i.e., infection is present) for each strain.

Table 4. Numbers of mice evaluated for each of 19 CC strains are shown, separated by sex and infection status. Average levels of TMEV RNA detected in infected mice at 90 dpi, compared to sham-infected mice of the same strain, are reported in the column "TMEV 90 dpi." We considered negative values to indicate undetectable levels of TMEV RNA. The average 90 dpi cumulative scores for infected mice of each strain (as previously reported, [23]) are listed in the far-right column. Note that phenotypes of sham-infected mice were also evaluated, and used as baseline when scoring infected mice of the same sex and strain.

Strain	Infected F	Infected M	Sham F	Sham M	Total *n*	TMEV 90 dpi	90 dpi Cumulative Score
CC002	1	2	1	1	5	−1.52	1.08
CC005	2	4	3	3	12	21.90	2.18
CC006	3	2	4	2	11	23.98	0.60
CC011	3	4	3	3	13	22.55	1.68
CC015	1	2	1	2	6	32.38	0.45
CC017	1	3	2	3	9	27.56	1.34
CC023	1	1	3	2	7	20.95	3.61
CC024	1	1	1	0	3	0.15	0.95
CC025	1	1	1	0	3	−1.24	1.21
CC027	3	1	2	3	9	24.72	0.27
CC032×CC013	2	4	1	1	8	−3.60	0.61
CC036	1	6	1	2	10	−11.25	0.69
CC037	3	4	2	3	12	21.53	0.61
CC041	2	2	2	0	6	0.29	1.34
CC041×CC012	5	4	2	1	12	20.85	1.35
CC043	0	2	1	1	4	20.79	0.84
CC051	5	1	2	1	9	−2.67	0.28
CC058	1	0	1	1	3	4.48	1.81
CC072	0	2	1	0	3	4.60	2.08
Total	36	46	34	29	145		

4.3. Identification of Key Pathways, Networks, and Regulatory Molecules

Ingenuity Pathways Analysis (IPA) software was used to evaluate gene expression data, identifying key networks and pathways for each individual strain, for all strains combined, and for groups of strains (specifically resistant, resilient, and susceptible response groups). The "overall" group included all mice in the study. For analyses specific to TMEV response groups, resistant strains included all mice from CC002, CC032×CC013, CC036, and CC051; resilient strains included all mice from CC006, CC015, CC027, CC037, and CC043; susceptible mice included all mice from strain CC023. Strains for which categorization varied by sex (e.g., CC024 and CC041), or TMEV response groups represented by all members of only one strain (e.g., intermediate [CC041×CC012], intractable [CC058], and refractory [CC072]), or strains which represented more than one response group (e.g., CC005, CC011, and CC017) were not included in response group-specific evaluations.

Target molecules regulated by the top genes and proteins governing each network/pathway were also identified. Biomarkers were identified for each response group using IPA's Biomarker Filter function.

IPA calculates *p*-values differently depending on the analysis, as described [28]. In general, significance was determined using Fisher's Exact Test. We applied the Benjamini–Hochberg method for multiple testing correction when identifying significant Canonical Pathways, Upstream Regulators, Networks, and Diseases/Functions.

4.4. Haplotypes and Sequence Variation

Haplotypes for loci of interest were identified using the Collaborative Cross Viewer [138,139]. SNPs within these loci were identified by querying two separate datasets: Sanger4 (for CC founder strains) and UNC-GMUGA1 (for CC strains and founder strains) [140,141] via the Mouse Phenome Database (MPD) (RRID:SCR_003212) [142]. Additionally,

the Mouse Genomes Project was queried for SNPs, insertion/deletion variants (indels), and structural variants within and near loci of interest for CC founder strain genomes [143,144].

5. Conclusions

This study revealed a novel outcome for TMEV infection: resilience, which has features of both resistance and susceptibility to infection. Gene expression analysis allowed the comparison of pathways and networks involved in different TMEV outcome categories, which were distinguished from each other by collecting phenotype data from 19 genetically diverse mouse strains over 90 days post-infection. Expression profiling of resistant, resilient, and susceptible mouse strains revealed functionally relevant genetic variation, such as sequence-level differences in non-coding RNAs and miRNAs, which modulate gene expression and interactivity.

Supplementary Materials: The following are available online at https://www.mdpi.com/article/10.3390/ijms222111379/s1.

Author Contributions: Conceptualization, C.B.-L., C.J.W., D.W.T.; validation, K.K.; formal analysis, K.K., A.H.; investigation, K.A., K.L., A.P.-G., C.R.Y.; resources, C.J.W., D.W.T.; data curation, C.B.-L., K.A., K.L., A.P.-G.; writing—original draft preparation, C.B.-L.; writing—review and editing, D.W.T., C.J.W., C.R.Y.; visualization, C.B.-L.; supervision, C.B.-L.; project administration, C.B.-L.; funding acquisition, C.B.-L. All authors have read and agreed to the published version of the manuscript.

Funding: This research was funded by the National Institute of Neurological Disorders and Stroke, grant number R01 NS103934 and supported by resources at the Texas A&M Center for Environmental Health Research (National Institute of Environmental Health Sciences grant number P30 ES029067).

Institutional Review Board Statement: The study was approved by the Institutional Review Board of Texas A&M University (protocol codes 2017-0082, approved 20 July 2017, and 2020-0065, approved 21 May 2020).

Informed Consent Statement: Not applicable.

Data Availability Statement: The data presented in this article are available in Supplementary Materials.

Acknowledgments: The authors acknowledge Raena Eldridge, Austen Herron, Xing Zhang, and other undergraduate students who assisted with tissue collection and RNA extraction, purification, and quality checking. We also acknowledge Ivan Ivanov and Destiny McNeece-Mullens for training in using IPA.

Conflicts of Interest: The authors declare no conflict of interest. The funders had no role in the design of the study; in the collection, analyses, or interpretation of data; in the writing of the manuscript, or in the decision to publish the results.

References

1. Threadgill, D.W.; Hunter, K.W.; Williams, R.W. Genetic dissection of complex and quantitative traits: From fantasy to reality via a community effort. *Mamm. Genome* **2002**, *13*, 175–178. [CrossRef] [PubMed]
2. Threadgill, D.W.; Miller, D.R.; Churchill, G.A.; de Villena, F.P. The collaborative cross: A recombinant inbred mouse population for the systems genetic era. *ILAR J.* **2011**, *52*, 24–31. [CrossRef] [PubMed]
3. Zou, F.; Gelfond, J.A.; Airey, D.C.; Lu, L.; Manly, K.F.; Williams, R.W.; Threadgill, D.W. Quantitative trait locus analysis using recombinant inbred intercrosses: Theoretical and empirical considerations. *Genetics* **2005**, *170*, 1299–1311. [CrossRef] [PubMed]
4. Brahic, M.; Bureau, J.F.; Michiels, T. The genetics of the persistent infection and demyelinating disease caused by Theiler's virus. *Annu. Rev. Microbiol.* **2005**, *59*, 279–298. [CrossRef]
5. Butterfield, R.J.; Roper, R.J.; Rhein, D.M.; Melvold, R.W.; Haynes, L.; Ma, R.Z.; Doerge, R.W.; Teuscher, C. Sex-specific quantitative trait loci govern susceptibility to Theiler's murine encephalomyelitis virus-induced demyelination. *Genetics* **2003**, *163*, 1041–1046. [CrossRef]
6. Clatch, R.J.; Melvold, R.W.; Miller, S.D.; Lipton, H.L. Theiler's murine encephalomyelitis virus (TMEV)-induced demyelinating disease in mice is influenced by the H-2D region: Correlation with TEMV-specific delayed-type hypersensitivity. *J. Immunol.* **1985**, *135*, 1408–1414.
7. Fiette, L.; Aubert, C.; Muller, U.; Huang, S.; Aguet, M.; Brahic, M.; Bureau, J.F. Theiler's virus infection of 129Sv mice that lack the interferon alpha/beta or interferon gamma receptors. *J. Exp. Med.* **1995**, *181*, 2069–2076. [CrossRef]

8. Rodriguez, M.; David, C.S. Demyelination induced by Theiler's virus: Influence of the H-2 haplotype. *J. Immunol.* **1985**, *135*, 2145–2148.
9. Rodriguez, M.; Leibowitz, J.; David, C.S. Susceptibility to Theiler's virus-induced demyelination. Mapping of the gene within the H-2D region. *J. Exp. Med.* **1986**, *163*, 620–631.
10. Levillayer, F.; Mas, M.; Levi-Acobas, F.; Brahic, M.; Bureau, J.F. Interleukin 22 is a candidate gene for Tmevp3, a locus controlling Theiler's virus-induced neurological diseases. *Genetics* **2007**, *176*, 1835–1844. [CrossRef]
11. Aubagnac, S.; Brahic, M.; Bureau, J.F. Viral load and a locus on chromosome 11 affect the late clinical disease caused by Theiler's virus. *J. Virol.* **1999**, *73*, 7965–7971. [CrossRef]
12. Bieber, A.J.; Suwansrinon, K.; Kerkvliet, J.; Zhang, W.; Pease, L.R.; Rodriguez, M. Allelic variation in the Tyk2 and EGF genes as potential genetic determinants of CNS repair. *Proc. Natl. Acad. Sci. USA* **2010**, *107*, 792–797. [CrossRef]
13. Bihl, F.; Brahic, M.; Bureau, J.F. Two loci, Tmevp2 and Tmevp3, located on the telomeric region of chromosome 10, control the persistence of Theiler's virus in the central nervous system of mice. *Genetics* **1999**, *152*, 385–392. [CrossRef] [PubMed]
14. Brahic, M.; Bureau, J.F. Genetics of susceptibility to Theiler's virus infection. *Bioessays* **1998**, *20*, 627–633. [CrossRef]
15. Bureau, J.F.; Drescher, K.M.; Pease, L.R.; Vikoren, T.; Delcroix, M.; Zoecklein, L.; Brahic, M.; Rodriguez, M. Chromosome 14 contains determinants that regulate susceptibility to Theiler's virus-induced demyelination in the mouse. *Genetics* **1998**, *148*, 1941–1949. [CrossRef] [PubMed]
16. Melvold, R.W.; Jokinen, D.M.; Knobler, R.L.; Lipton, H.L. Variations in genetic control of susceptibility to Theiler's murine encephalomyelitis virus (TMEV)-induced demyelinating disease. I. Differences between susceptible SJL/J and resistant BALB/c strains map near the T cell beta-chain constant gene on chromosome 6. *J. Immunol.* **1987**, *138*, 1429–1433.
17. Melvold, R.W.; Jokinen, D.M.; Miller, S.D.; Dal Canto, M.C.; Lipton, H.L. Identification of a locus on mouse chromosome 3 involved in differential susceptibility to Theiler's murine encephalomyelitis virus-induced demyelinating disease. *J. Virol.* **1990**, *64*, 686–690. [CrossRef] [PubMed]
18. Teuscher, C.; Rhein, D.M.; Livingstone, K.D.; Paynter, R.A.; Doerge, R.W.; Nicholson, S.M.; Melvold, R.W. Evidence that Tmevd2 and eae3 may represent either a common locus or members of a gene complex controlling susceptibility to immunologically mediated demyelination in mice. *J. Immunol.* **1997**, *159*, 4930–4934.
19. Bureau, J.F.; Montagutelli, X.; Bihl, F.; Lefebvre, S.; Guenet, J.L.; Brahic, M. Mapping loci influencing the persistence of Theiler's virus in the murine central nervous system. *Nat. Genet.* **1993**, *5*, 87–91. [CrossRef]
20. Lipton, H.L.; Melvold, R. Genetic analysis of susceptibility to Theiler's virus-induced demyelinating disease in mice. *J. Immunol.* **1984**, *132*, 1821–1825.
21. Khan, M.R.; Wellinger, R.J.; Laurent, B. Exploring the Alternative Splicing of Long Noncoding RNAs. *Trends Genet.* **2021**. [CrossRef]
22. Sun, L.; Goff, L.A.; Trapnell, C.; Alexander, R.; Lo, K.A.; Hacisuleyman, E.; Sauvageau, M.; Tazon-Vega, B.; Kelley, D.R.; Hendrickson, D.G.; et al. Long noncoding RNAs regulate adipogenesis. *Proc. Natl. Acad. Sci. USA* **2013**, *110*, 3387–3392. [CrossRef]
23. Eldridge, R.; Osorio, D.; Amstalden, K.; Edwards, C.; Young, C.R.; Cai, J.J.; Konganti, K.; Hillhouse, A.; Threadgill, D.W.; Welsh, C.J.; et al. Antecedent presentation of neurological phenotypes in the Collaborative Cross reveals four classes with complex sex-dependencies. *Sci. Rep.* **2020**, *10*, 7918. [CrossRef]
24. Lipton, H.L.; Dal Canto, M.C. Susceptibility of inbred mice to chronic central nervous system infection by Theiler's murine encephalomyelitis virus. *Infect. Immun.* **1979**, *26*, 369–374. [CrossRef] [PubMed]
25. Clatch, R.J.; Lipton, H.L.; Miller, S.D. Class II-restricted T cell responses in Theiler's murine encephalomyelitis virus (TMEV)-induced demyelinating disease. II. Survey of host immune responses and central nervous system virus titers in inbred mouse strains. *Microb. Pathog.* **1987**, *3*, 327–337. [CrossRef]
26. Klein, J.P.; Sun, Z.; Staff, N.P. Association between ALS and retroviruses: Evidence from bioinformatics analysis. *BMC Bioinform.* **2019**, *20*, 680. [CrossRef] [PubMed]
27. Juranic Lisnic, V.; Babic Cac, M.; Lisnic, B.; Trsan, T.; Mefferd, A.; Das Mukhopadhyay, C.; Cook, C.H.; Jonjic, S.; Trgovcich, J. Dual analysis of the murine cytomegalovirus and host cell transcriptomes reveal new aspects of the virus-host cell interface. *PLoS Pathog.* **2013**, *9*, e1003611. [CrossRef]
28. Calculating and Interpreting the p-values for Functions, Pathways, and Lists in IPA; Qiagen: Germantown, MD, USA. 2010. Available online: https://qiagen.secure.force.com/KnowledgeBase/KnowledgeIPAPage?id=kA41i000000L5nQCAS (accessed on 14 October 2021).
29. Kramer, A.; Green, J.; Pollard, J., Jr.; Tugendreich, S. Causal analysis approaches in Ingenuity Pathway Analysis. *Bioinformatics* **2014**, *30*, 523–530. [CrossRef]
30. Li Puma, D.D.; Piacentini, R.; Leone, L.; Gironi, K.; Marcocci, M.E.; De Chiara, G.; Palamara, A.T.; Grassi, C. Herpes Simplex Virus Type-1 Infection Impairs Adult Hippocampal Neurogenesis via Amyloid-beta Protein Accumulation. *Stem Cells* **2019**, *37*, 1467–1480. [CrossRef]
31. Hagg, E.; Astrom, L.; Steen, L. Persistent hypothalamic-pituitary insufficiency following acute meningoencephalitis. A report of two cases. *Acta Med. Scand.* **1978**, *203*, 231–235. [CrossRef]
32. Kupari, M.; Pelkonen, R.; Valtonen, V. Post-encephalitic hypothalamic-pituitary insufficiency. *Acta Endocrinol. (Copenh.)* **1980**, *94*, 433–438. [CrossRef]

33. Beatrice, A.M.; Selvan, C.; Mukhopadhyay, S. Pituitary dysfunction in infective brain diseases. *Indian J. Endocrinol. Metab.* **2013**, *17*, S608–S611. [CrossRef] [PubMed]
34. Tanriverdi, F.; De Bellis, A.; Teksahin, H.; Alp, E.; Bizzarro, A.; Sinisi, A.A.; Bellastella, G.; Paglionico, V.A.; Bellastella, A.; Unluhizarci, K.; et al. Prospective investigation of pituitary functions in patients with acute infectious meningitis: Is acute meningitis induced pituitary dysfunction associated with autoimmunity? *Pituitary* **2012**, *15*, 579–588. [CrossRef]
35. Sarasin-Filipowicz, M.; Krol, J.; Markiewicz, I.; Heim, M.H.; Filipowicz, W. Decreased levels of microRNA miR-122 in individuals with hepatitis C responding poorly to interferon therapy. *Nat. Med.* **2009**, *15*, 31–33. [CrossRef] [PubMed]
36. Israelow, B.; Narbus, C.M.; Sourisseau, M.; Evans, M.J. HepG2 cells mount an effective antiviral interferon-lambda based innate immune response to hepatitis C virus infection. *Hepatology* **2014**, *60*, 1170–1179. [CrossRef]
37. Accessing and Using Upstream Regulators; QIAGEN Digital Insights: Germantown, MD, USA. 2021. Available online: https://qiagen.secure.force.com/KnowledgeBase/KnowledgeIPAPage?id=kA41i000000L5sECAS (accessed on 14 October 2021).
38. Vazirinejad, R.; Ahmadi, Z.; Kazemi Arababadi, M.; Hassanshahi, G.; Kennedy, D. The biological functions, structure and sources of CXCL10 and its outstanding part in the pathophysiology of multiple sclerosis. *Neuroimmunomodulation* **2014**, *21*, 322–330. [CrossRef]
39. Djelloul, M.; Popa, N.; Pelletier, F.; Raguenez, G.; Boucraut, J. RAE-1 expression is induced during experimental autoimmune encephalomyelitis and is correlated with microglia cell proliferation. *Brain Behav. Immun.* **2016**, *58*, 209–217. [CrossRef]
40. Arapovic, J.; Lenac, T.; Antulov, R.; Polic, B.; Ruzsics, Z.; Carayannopoulos, L.N.; Koszinowski, U.H.; Krmpotic, A.; Jonjic, S. Differential susceptibility of RAE-1 isoforms to mouse cytomegalovirus. *J. Virol.* **2009**, *83*, 8198–8207. [CrossRef]
41. Spreafico, A.; Delord, J.P.; De Mattos-Arruda, L.; Berge, Y.; Rodon, J.; Cottura, E.; Bedard, P.L.; Akimov, M.; Lu, H.; Pain, S.; et al. A first-in-human phase I, dose-escalation, multicentre study of HSP990 administered orally in adult patients with advanced solid malignancies. *Br. J. Cancer* **2015**, *112*, 650–659. [CrossRef]
42. Mutsvunguma, L.Z.; Moetlhoa, B.; Edkins, A.L.; Luke, G.A.; Blatch, G.L.; Knox, C. Theiler's murine encephalomyelitis virus infection induces a redistribution of heat shock proteins 70 and 90 in BHK-21 cells, and is inhibited by novobiocin and geldanamycin. *Cell Stress Chaperones* **2011**, *16*, 505–515. [CrossRef]
43. Ross, C.; Upfold, N.; Luke, G.A.; Bishop, O.T.; Knox, C. Subcellular localisation of Theiler's murine encephalomyelitis virus (TMEV) capsid subunit VP1 vis-a-vis host protein Hsp90. *Virus Res.* **2016**, *222*, 53–63. [CrossRef]
44. Eaton, A.; Bernier, F.P.; Goedhart, C.; Caluseriu, O.; Lamont, R.E.; Boycott, K.M.; Parboosingh, J.S.; Innes, A.M.; Care4Rare Canada, C. Is PNPT1-related hearing loss ever non-syndromic? Whole exome sequencing of adult siblings expands the natural history of PNPT1-related disorders. *Am. J. Med. Genet. A* **2018**, *176*, 2487–2493. [CrossRef] [PubMed]
45. Sato, R.; Arai-Ichinoi, N.; Kikuchi, A.; Matsuhashi, T.; Numata-Uematsu, Y.; Uematsu, M.; Fujii, Y.; Murayama, K.; Ohtake, A.; Abe, T.; et al. Novel biallelic mutations in the PNPT1 gene encoding a mitochondrial-RNA-import protein PNPase cause delayed myelination. *Clin. Genet.* **2018**, *93*, 242–247. [CrossRef] [PubMed]
46. Hunn, J.P.; Howard, J.C. The mouse resistance protein Irgm1 (LRG-47): A regulator or an effector of pathogen defense? *PLoS Pathog.* **2010**, *6*, e1001008. [CrossRef] [PubMed]
47. Maric-Biresev, J.; Hunn, J.P.; Krut, O.; Helms, J.B.; Martens, S.; Howard, J.C. Loss of the interferon-gamma-inducible regulatory immunity-related GTPase (IRG), Irgm1, causes activation of effector IRG proteins on lysosomes, damaging lysosomal function and predicting the dramatic susceptibility of Irgm1-deficient mice to infection. *BMC Biol.* **2016**, *14*, 33. [CrossRef]
48. Rai, P.; Janardhan, K.S.; Meacham, J.; Madenspacher, J.H.; Lin, W.C.; Karmaus, P.W.F.; Martinez, J.; Li, Q.Z.; Yan, M.; Zeng, J.; et al. IRGM1 links mitochondrial quality control to autoimmunity. *Nat. Immunol.* **2021**, *22*, 312–321. [CrossRef] [PubMed]
49. Yao, Q.M.; Zhu, Y.F.; Wang, W.; Song, Z.Y.; Shao, X.Q.; Li, L.; Song, R.H.; An, X.F.; Qin, Q.; Li, Q.; et al. Polymorphisms in Autophagy-Related Gene IRGM Are Associated with Susceptibility to Autoimmune Thyroid Diseases. *Biomed. Res. Int.* **2018**, *2018*, 7959707. [CrossRef] [PubMed]
50. Crow, M.K. Type I interferon in organ-targeted autoimmune and inflammatory diseases. *Arthritis Res. Ther.* **2010**, *12* (Suppl. 1), S5. [CrossRef]
51. Li, S.F.; Gong, M.J.; Zhao, F.R.; Shao, J.J.; Xie, Y.L.; Zhang, Y.G.; Chang, H.Y. Type I Interferons: Distinct Biological Activities and Current Applications for Viral Infection. *Cell Physiol. Biochem.* **2018**, *51*, 2377–2396. [CrossRef]
52. Christodoulou-Vafeiadou, E.; Ioakeimidis, F.; Andreadou, M.; Giagkas, G.; Stamatakis, G.; Reczko, M.; Samiotaki, M.; Papanastasiou, A.D.; Karakasiliotis, I.; Kontoyiannis, D.L. Divergent Innate and Epithelial Functions of the RNA-Binding Protein HuR in Intestinal Inflammation. *Front. Immunol.* **2018**, *9*, 2732. [CrossRef]
53. Kafasla, P.; Skliris, A.; Kontoyiannis, D.L. Post-transcriptional coordination of immunological responses by RNA-binding proteins. *Nat. Immunol.* **2014**, *15*, 492–502. [CrossRef] [PubMed]
54. Unterholzner, L.; Keating, S.E.; Baran, M.; Horan, K.A.; Jensen, S.B.; Sharma, S.; Sirois, C.M.; Jin, T.; Latz, E.; Xiao, T.S.; et al. IFI16 is an innate immune sensor for intracellular DNA. *Nat. Immunol.* **2010**, *11*, 997–1004. [CrossRef]
55. Molineros, J.E.; Maiti, A.K.; Sun, C.; Looger, L.L.; Han, S.; Kim-Howard, X.; Glenn, S.; Adler, A.; Kelly, J.A.; Niewold, T.B.; et al. Admixture mapping in lupus identifies multiple functional variants within IFIH1 associated with apoptosis, inflammation, and autoantibody production. *PLoS Genet.* **2013**, *9*, e1003222. [CrossRef] [PubMed]
56. Green, R.; Wilkins, C.; Thomas, S.; Sekine, A.; Hendrick, D.M.; Voss, K.; Ireton, R.C.; Mooney, M.; Go, J.T.; Choonoo, G.; et al. Oas1b-dependent Immune Transcriptional Profiles of West Nile Virus Infection in the Collaborative Cross. *G3 (Bethesda)* **2017**, *7*, 1665–1682. [CrossRef] [PubMed]

57. Kreit, M.; Vertommen, D.; Gillet, L.; Michiels, T. The Interferon-Inducible Mouse Apolipoprotein L9 and Prohibitins Cooperate to Restrict Theiler's Virus Replication. *PLoS ONE* **2015**, *10*, e0133190. [CrossRef] [PubMed]
58. Nordmann, A.; Wixler, L.; Boergeling, Y.; Wixler, V.; Ludwig, S. A new splice variant of the human guanylate-binding protein 3 mediates anti-influenza activity through inhibition of viral transcription and replication. *FASEB J.* **2012**, *26*, 1290–1300. [CrossRef]
59. Florio, T.; Barbieri, F.; Spaziante, R.; Zona, G.; Hofland, L.J.; van Koetsveld, P.M.; Feelders, R.A.; Stalla, G.K.; Theodoropoulou, M.; Culler, M.D.; et al. Efficacy of a dopamine-somatostatin chimeric molecule, BIM-23A760, in the control of cell growth from primary cultures of human non-functioning pituitary adenomas: A multi-center study. *Endocr. Relat. Cancer* **2008**, *15*, 583–596. [CrossRef]
60. Ibanez-Costa, A.; Lopez-Sanchez, L.M.; Gahete, M.D.; Rivero-Cortes, E.; Vazquez-Borrego, M.C.; Galvez, M.A.; de la Riva, A.; Venegas-Moreno, E.; Jimenez-Reina, L.; Moreno-Carazo, A.; et al. BIM-23A760 influences key functional endpoints in pituitary adenomas and normal pituitaries: Molecular mechanisms underlying the differential response in adenomas. *Sci. Rep.* **2017**, *7*, 42002. [CrossRef]
61. Jaquet, P.; Gunz, G.; Saveanu, A.; Barlier, A.; Dufour, H.; Taylor, J.; Dong, J.; Kim, S.; Moreau, J.P.; Culler, M.D. BIM-23A760, a chimeric molecule directed towards somatostatin and dopamine receptors, vs universal somatostatin receptors ligands in GH-secreting pituitary adenomas partial responders to octreotide. *J. Endocrinol. Investig.* **2005**, *28*, 21–27.
62. Li, K.; Ma, Y.B.; Zhang, Z.; Tian, Y.H.; Xu, X.L.; He, Y.Q.; Xu, L.; Gao, Y.; Pan, W.T.; Song, W.J.; et al. Upregulated IQUB promotes cell proliferation and migration via activating Akt/GSK3beta/beta-catenin signaling pathway in breast cancer. *Cancer Med.* **2018**, *7*, 3875–3888. [CrossRef]
63. Tanabe, K.; Tachibana, T.; Yamashita, T.; Che, Y.H.; Yoneda, Y.; Ochi, T.; Tohyama, M.; Yoshikawa, H.; Kiyama, H. The small GTP-binding protein TC10 promotes nerve elongation in neuronal cells, and its expression is induced during nerve regeneration in rats. *J. Neurosci.* **2000**, *20*, 4138–4144. [CrossRef] [PubMed]
64. Abe, T.; Kato, M.; Miki, H.; Takenawa, T.; Endo, T. Small GTPase Tc10 and its homologue RhoT induce N-WASP-mediated long process formation and neurite outgrowth. *J. Cell Sci.* **2003**, *116*, 155–168. [CrossRef] [PubMed]
65. Burbage, M.; Keppler, S.J.; Montaner, B.; Mattila, P.K.; Batista, F.D. The Small Rho GTPase TC10 Modulates B Cell Immune Responses. *J. Immunol.* **2017**, *199*, 1682–1695. [CrossRef]
66. Sheng, Y.; Hong, J.H.; Doherty, R.; Srikumar, T.; Shloush, J.; Avvakumov, G.V.; Walker, J.R.; Xue, S.; Neculai, D.; Wan, J.W.; et al. A human ubiquitin conjugating enzyme (E2)-HECT E3 ligase structure-function screen. *Mol. Cell Proteom.* **2012**, *11*, 329–341. [CrossRef] [PubMed]
67. Hu, N.; Xie, X.C.; Liu, L.L.; Lai, W.D. Aberrant methylation of UBE2Q1 promoter is associated with poor prognosis of acute-on-chronic hepatitis B pre-liver failure. *Medicine* **2021**, *100*, e26066. [CrossRef] [PubMed]
68. Hu, N.; Fan, X.P.; Fan, Y.C.; Chen, L.Y.; Qiao, C.Y.; Han, L.Y.; Wang, K. Hypomethylated Ubiquitin-Conjugating Enzyme2 Q1 (UBE2Q1) Gene Promoter in the Serum Is a Promising Biomarker for Hepatitis B Virus-Associated Hepatocellular Carcinoma. *Tohoku J. Exp. Med.* **2017**, *242*, 93–100. [CrossRef] [PubMed]
69. Zhang, B.; Deng, C.; Wang, L.; Zhou, F.; Zhang, S.; Kang, W.; Zhan, P.; Chen, J.; Shen, S.; Guo, H.; et al. Upregulation of UBE2Q1 via gene copy number gain in hepatocellular carcinoma promotes cancer progression through beta-catenin-EGFR-PI3K-Akt-mTOR signaling pathway. *Mol. Carcinog.* **2018**, *57*, 201–215. [CrossRef] [PubMed]
70. Topno, R.; Singh, I.; Kumar, M.; Agarwal, P. Integrated bioinformatic analysis identifies UBE2Q1 as a potential prognostic marker for high grade serous ovarian cancer. *BMC Cancer* **2021**, *21*, 220. [CrossRef] [PubMed]
71. Grzmil, P.; Altmann, M.E.; Adham, I.M.; Engel, U.; Jarry, H.; Schweyer, S.; Wolf, S.; Manz, J.; Engel, W. Embryo implantation failure and other reproductive defects in Ube2q1-deficient female mice. *Reproduction* **2013**, *145*, 45–56. [CrossRef]
72. Belli, M.; Shimasaki, S. Molecular Aspects and Clinical Relevance of GDF9 and BMP15 in Ovarian Function. *Vitam. Horm.* **2018**, *107*, 317–348. [CrossRef]
73. Sanfins, A.; Rodrigues, P.; Albertini, D.F. GDF-9 and BMP-15 direct the follicle symphony. *J. Assist. Reprod. Genet.* **2018**, *35*, 1741–1750. [CrossRef]
74. Leung, Y.T.; Maurer, K.; Song, L.; Convissar, J.; Sullivan, K.E. Prolactin activates IRF1 and leads to altered balance of histone acetylation: Implications for systemic lupus erythematosus. *Mod. Rheumatol.* **2020**, *30*, 532–543. [CrossRef]
75. Tufa, D.M.; Shank, T.; Yingst, A.M.; Trahan, G.D.; Shim, S.; Lake, J.; Woods, R.; Jones, K.; Verneris, M.R. Prolactin Acts on Myeloid Progenitors to Modulate SMAD7 Expression and Enhance Hematopoietic Stem Cell Differentiation into the NK Cell Lineage. *Sci. Rep.* **2020**, *10*, 6335. [CrossRef]
76. Falcon, A.M.; Fortes, P.; Marion, R.M.; Beloso, A.; Ortin, J. Interaction of influenza virus NS1 protein and the human homologue of Staufen in vivo and in vitro. *Nucl. Acids Res.* **1999**, *27*, 2241–2247. [CrossRef]
77. Chatel-Chaix, L.; Boulay, K.; Mouland, A.J.; Desgroseillers, L. The host protein Staufen1 interacts with the Pr55Gag zinc fingers and regulates HIV-1 assembly via its N-terminus. *Retrovirology* **2008**, *5*, 41. [CrossRef]
78. Hanke, K.; Hohn, O.; Liedgens, L.; Fiddeke, K.; Wamara, J.; Kurth, R.; Bannert, N. Staufen-1 interacts with the human endogenous retrovirus family HERV-K(HML-2) rec and gag proteins and increases virion production. *J. Virol.* **2013**, *87*, 11019–11030. [CrossRef] [PubMed]
79. Fang, J.; Pietzsch, C.; Ramanathan, P.; Santos, R.I.; Ilinykh, P.A.; Garcia-Blanco, M.A.; Bukreyev, A.; Bradrick, S.S. Staufen1 Interacts with Multiple Components of the Ebola Virus Ribonucleoprotein and Enhances Viral RNA Synthesis. *mBio* **2018**, *9*, e01771-18. [CrossRef] [PubMed]

80. Lu, J.; Clark, A.G. Impact of microRNA regulation on variation in human gene expression. *Genome Res.* **2012**, *22*, 1243–1254. [CrossRef] [PubMed]
81. Cammaerts, S.; Strazisar, M.; De Rijk, P.; Del Favero, J. Genetic variants in microRNA genes: Impact on microRNA expression, function, and disease. *Front. Genet.* **2015**, *6*, 186. [CrossRef]
82. Kozomara, A.; Birgaoanu, M.; Griffiths-Jones, S. miRBase: From microRNA sequences to function. *Nucl. Acids Res.* **2019**, *47*, D155–D162. [CrossRef] [PubMed]
83. Pollio, G.; Hoozemans, J.J.; Andersen, C.A.; Roncarati, R.; Rosi, M.C.; van Haastert, E.S.; Seredenina, T.; Diamanti, D.; Gotta, S.; Fiorentini, A.; et al. Increased expression of the oligopeptidase THOP1 is a neuroprotective response to Abeta toxicity. *Neurobiol. Dis.* **2008**, *31*, 145–158. [CrossRef]
84. Sundstrom, J.M.; Hernandez, C.; Weber, S.R.; Zhao, Y.; Dunklebarger, M.; Tiberti, N.; Laremore, T.; Simo-Servat, O.; Garcia-Ramirez, M.; Barber, A.J.; et al. Proteomic Analysis of Early Diabetic Retinopathy Reveals Mediators of Neurodegenerative Brain Diseases. *Investig. Ophthalmol. Vis. Sci.* **2018**, *59*, 2264–2274. [CrossRef] [PubMed]
85. Brinkmeyer-Langford, C.L.; Rech, R.; Amstalden, K.; Kochan, K.J.; Hillhouse, A.E.; Young, C.; Welsh, C.J.; Threadgill, D.W. Host genetic background influences diverse neurological responses to viral infection in mice. *Sci. Rep.* **2017**, *7*, 12194. [CrossRef]
86. Carneiro-Sampaio, M.; Coutinho, A. Tolerance and autoimmunity: Lessons at the bedside of primary immunodeficiencies. *Adv. Immunol.* **2007**, *95*, 51–82. [CrossRef]
87. Azizi, G.; Ghanavatinejad, A.; Abolhassani, H.; Yazdani, R.; Rezaei, N.; Mirshafiey, A.; Aghamohammadi, A. Autoimmunity in primary T-cell immunodeficiencies. *Expert Rev. Clin. Immunol.* **2016**, *12*, 989–1006. [CrossRef]
88. Comrie, W.A.; Lenardo, M.J. Molecular Classification of Primary Immunodeficiencies of T Lymphocytes. *Adv. Immunol.* **2018**, *138*, 99–193. [CrossRef] [PubMed]
89. Mackay, I.R.; Leskovsek, N.V.; Rose, N.R. The odd couple: A fresh look at autoimmunity and immunodeficiency. *J. Autoimmun* **2010**, *35*, 199–205. [CrossRef] [PubMed]
90. Todoric, K.; Koontz, J.B.; Mattox, D.; Tarrant, T.K. Autoimmunity in immunodeficiency. *Curr. Allergy Asthma Rep.* **2013**, *13*, 361–370. [CrossRef] [PubMed]
91. Kawai, T.; Akira, S. The role of pattern-recognition receptors in innate immunity: Update on Toll-like receptors. *Nat. Immunol.* **2010**, *11*, 373–384. [CrossRef]
92. Thompson, M.R.; Kaminski, J.J.; Kurt-Jones, E.A.; Fitzgerald, K.A. Pattern recognition receptors and the innate immune response to viral infection. *Viruses* **2011**, *3*, 920–940. [CrossRef]
93. Gerhauser, I.; Hansmann, F.; Ciurkiewicz, M.; Loscher, W.; Beineke, A. Facets of Theiler's Murine Encephalomyelitis Virus-Induced Diseases: An Update. *Int. J. Mol. Sci.* **2019**, *20*. [CrossRef]
94. Turrin, N.P. Central nervous system Toll-like receptor expression in response to Theiler's murine encephalomyelitis virus-induced demyelination disease in resistant and susceptible mouse strains. *Virol. J.* **2008**, *5*, 154. [CrossRef]
95. Nicholson, S.M.; Peterson, J.D.; Miller, S.D.; Wang, K.; Dal Canto, M.C.; Melvold, R.W. BALB/c substrain differences in susceptibility to Theiler's murine encephalomyelitis virus-induced demyelinating disease. *J. Neuroimmunol.* **1994**, *52*, 19–24. [CrossRef]
96. Jordan, N.V.; Johnson, G.L.; Abell, A.N. Tracking the intermediate stages of epithelial-mesenchymal transition in epithelial stem cells and cancer. *Cell Cycle* **2011**, *10*, 2865–2873. [CrossRef]
97. Yasuda, K.; Torigoe, T.; Mariya, T.; Asano, T.; Kuroda, T.; Matsuzaki, J.; Ikeda, K.; Yamauchi, M.; Emori, M.; Asanuma, H.; et al. Fibroblasts induce expression of FGF4 in ovarian cancer stem-like cells/cancer-initiating cells and upregulate their tumor initiation capacity. *Lab. Investig.* **2014**, *94*, 1355–1369. [CrossRef] [PubMed]
98. Zhang, Y.W.; Liu, S.; Zhang, X.; Li, W.B.; Chen, Y.; Huang, X.; Sun, L.; Luo, W.; Netzer, W.J.; Threadgill, R.; et al. A functional mouse retroposed gene Rps23r1 reduces Alzheimer's beta-amyloid levels and tau phosphorylation. *Neuron* **2009**, *64*, 328–340. [CrossRef] [PubMed]
99. Huang, X.; Chen, Y.; Li, W.B.; Cohen, S.N.; Liao, F.F.; Li, L.; Xu, H.; Zhang, Y.W. The Rps23rg gene family originated through retroposition of the ribosomal protein s23 mRNA and encodes proteins that decrease Alzheimer's beta-amyloid level and tau phosphorylation. *Hum. Mol. Genet.* **2010**, *19*, 3835–3843. [CrossRef]
100. Zhao, D.; Meng, J.; Zhao, Y.; Huo, Y.; Liu, Y.; Zheng, N.; Zhang, M.; Gao, Y.; Chen, Z.; Sun, H.; et al. RPS23RG1 Is Required for Synaptic Integrity and Rescues Alzheimer's Disease-Associated Cognitive Deficits. *Biol. Psychiatry* **2019**, *86*, 171–184. [CrossRef]
101. Boding, L.; Hansen, A.K.; Meroni, G.; Johansen, B.B.; Braunstein, T.H.; Bonefeld, C.M.; Kongsbak, M.; Jensen, B.A.; Woetmann, A.; Thomsen, A.R.; et al. Midline 1 directs lytic granule exocytosis and cytotoxicity of mouse killer T cells. *Eur J. Immunol.* **2014**, *44*, 3109–3118. [CrossRef] [PubMed]
102. Collison, A.; Hatchwell, L.; Verrills, N.; Wark, P.A.; de Siqueira, A.P.; Tooze, M.; Carpenter, H.; Don, A.S.; Morris, J.C.; Zimmermann, N.; et al. The E3 ubiquitin ligase midline 1 promotes allergen and rhinovirus-induced asthma by inhibiting protein phosphatase 2A activity. *Nat. Med.* **2013**, *19*, 232–237. [CrossRef]
103. Dorshkind, K.; Horseman, N.D. The roles of prolactin, growth hormone, insulin-like growth factor-I, and thyroid hormones in lymphocyte development and function: Insights from genetic models of hormone and hormone receptor deficiency. *Endocr. Rev.* **2000**, *21*, 292–312. [CrossRef] [PubMed]

104. Torner, L.; Karg, S.; Blume, A.; Kandasamy, M.; Kuhn, H.G.; Winkler, J.; Aigner, L.; Neumann, I.D. Prolactin prevents chronic stress-induced decrease of adult hippocampal neurogenesis and promotes neuronal fate. *J. Neurosci.* **2009**, *29*, 1826–1833. [CrossRef]
105. Walker, T.L.; Vukovic, J.; Koudijs, M.M.; Blackmore, D.G.; Mackay, E.W.; Sykes, A.M.; Overall, R.W.; Hamlin, A.S.; Bartlett, P.F. Prolactin stimulates precursor cells in the adult mouse hippocampus. *PLoS ONE* **2012**, *7*, e44371. [CrossRef] [PubMed]
106. Zhornitsky, S.; Johnson, T.A.; Metz, L.M.; Weiss, S.; Yong, V.W. Prolactin in combination with interferon-beta reduces disease severity in an animal model of multiple sclerosis. *J. Neuroinflamm.* **2015**, *12*, 55. [CrossRef]
107. Tang, M.W.; Garcia, S.; Gerlag, D.M.; Tak, P.P.; Reedquist, K.A. Insight into the Endocrine System and the Immune System: A Review of the Inflammatory Role of Prolactin in Rheumatoid Arthritis and Psoriatic Arthritis. *Front. Immunol.* **2017**, *8*, 720. [CrossRef]
108. Buskila, D.; Sukenik, S.; Shoenfeld, Y. The possible role of prolactin in autoimmunity. *Am. J. Reprod. Immunol.* **1991**, *26*, 118–123. [CrossRef]
109. Borba, V.V.; Zandman-Goddard, G.; Shoenfeld, Y. Prolactin and Autoimmunity. *Front. Immunol.* **2018**, *9*, 73. [CrossRef]
110. Correale, J.; Farez, M.F.; Ysrraelit, M.C. Role of prolactin in B cell regulation in multiple sclerosis. *J. Neuroimmunol.* **2014**, *269*, 76–86. [CrossRef]
111. Costanza, M.; Binart, N.; Steinman, L.; Pedotti, R. Prolactin: A versatile regulator of inflammation and autoimmune pathology. *Autoimmun. Rev.* **2015**, *14*, 223–230. [CrossRef]
112. Costanza, M.; Pedotti, R. Prolactin: Friend or Foe in Central Nervous System Autoimmune Inflammation? *Int. J. Mol. Sci.* **2016**, *17*. [CrossRef] [PubMed]
113. Parsons, R.B.; Smith, M.L.; Williams, A.C.; Waring, R.H.; Ramsden, D.B. Expression of nicotinamide N-methyltransferase (E.C. 2.1.1.1) in the Parkinsonian brain. *J. Neuropathol. Exp. Neurol.* **2002**, *61*, 111–124. [CrossRef]
114. Parsons, R.B.; Smith, S.W.; Waring, R.H.; Williams, A.C.; Ramsden, D.B. High expression of nicotinamide N-methyltransferase in patients with idiopathic Parkinson's disease. *Neurosci. Lett.* **2003**, *342*, 13–16. [CrossRef]
115. Schmeisser, K.; Parker, J.A. Nicotinamide-N-methyltransferase controls behavior, neurodegeneration and lifespan by regulating neuronal autophagy. *PLoS Genet.* **2018**, *14*, e1007561. [CrossRef] [PubMed]
116. Kocinaj, A.; Chaudhury, T.; Uddin, M.S.; Junaid, R.R.; Ramsden, D.B.; Hondhamuni, G.; Klamt, F.; Parsons, L.; Parsons, R.B. High Expression of Nicotinamide N-Methyltransferase in Patients with Sporadic Alzheimer's Disease. *Mol. Neurobiol.* **2021**, *58*, 1769–1781. [CrossRef] [PubMed]
117. Ramsden, D.B.; Waring, R.H.; Parsons, R.B.; Barlow, D.J.; Williams, A.C. Nicotinamide N-Methyltransferase: Genomic Connection to Disease. *Int. J. Tryptophan Res.* **2020**, *13*, 1178646920919770. [CrossRef] [PubMed]
118. Kraus, D.; Yang, Q.; Kong, D.; Banks, A.S.; Zhang, L.; Rodgers, J.T.; Pirinen, E.; Pulinilkunnil, T.C.; Gong, F.; Wang, Y.C.; et al. Nicotinamide N-methyltransferase knockdown protects against diet-induced obesity. *Nature* **2014**, *508*, 258–262. [CrossRef] [PubMed]
119. Bromberg, A.; Lerer, E.; Udawela, M.; Scarr, E.; Dean, B.; Belmaker, R.H.; Ebstein, R.; Agam, G. Nicotinamide-N-methyltransferase (NNMT) in schizophrenia: Genetic association and decreased frontal cortex mRNA levels. *Int. J. Neuropsychopharmacol.* **2012**, *15*, 727–737. [CrossRef]
120. Hu, Q.; Liu, F.; Yang, L.; Fang, Z.; He, J.; Wang, W.; You, P. Lower serum nicotinamide N-methyltransferase levels in patients with bipolar disorder during acute episodes compared to healthy controls: A cross-sectional study. *BMC Psychiatry* **2020**, *20*, 33. [CrossRef]
121. Milani, Z.H.; Ramsden, D.B.; Parsons, R.B. Neuroprotective effects of nicotinamide N-methyltransferase and its metabolite 1-methylnicotinamide. *J. Biochem. Mol. Toxicol.* **2013**, *27*, 451–456. [CrossRef]
122. Holwerda, S.J.; de Laat, W. CTCF: The protein, the binding partners, the binding sites and their chromatin loops. *Philos. Trans. R. Soc. Lond. B Biol. Sci.* **2013**, *368*, 20120369. [CrossRef]
123. Klenova, E.M.; Nicolas, R.H.; Paterson, H.F.; Carne, A.F.; Heath, C.M.; Goodwin, G.H.; Neiman, P.E.; Lobanenkov, V.V. CTCF, a conserved nuclear factor required for optimal transcriptional activity of the chicken c-myc gene, is an 11-Zn-finger protein differentially expressed in multiple forms. *Mol. Cell. Biol.* **1993**, *13*, 7612–7624. [CrossRef]
124. Ohlsson, R.; Renkawitz, R.; Lobanenkov, V. CTCF is a uniquely versatile transcription regulator linked to epigenetics and disease. *Trends Genet.* **2001**, *17*, 520–527. [CrossRef]
125. Phillips, J.E.; Corces, V.G. CTCF: Master weaver of the genome. *Cell* **2009**, *137*, 1194–1211. [CrossRef]
126. Sun, G.; Yan, J.; Noltner, K.; Feng, J.; Li, H.; Sarkis, D.A.; Sommer, S.S.; Rossi, J.J. SNPs in human miRNA genes affect biogenesis and function. *RNA* **2009**, *15*, 1640–1651. [CrossRef]
127. Shafi, G.; Aliya, N.; Munshi, A. MicroRNA signatures in neurological disorders. *Can. J. Neurol. Sci.* **2010**, *37*, 177–185. [CrossRef]
128. Christensen, M.; Schratt, G.M. microRNA involvement in developmental and functional aspects of the nervous system and in neurological diseases. *Neurosci. Lett.* **2009**, *466*, 55–62. [CrossRef]
129. Junn, E.; Mouradian, M.M. MicroRNAs in neurodegenerative diseases and their therapeutic potential. *Pharmacol. Ther.* **2012**, *133*, 142–150. [CrossRef] [PubMed]
130. Vohra, M.; Sharma, A.R.; Prabhu, B.N.; Rai, P.S. SNPs in Sites for DNA Methylation, Transcription Factor Binding, and miRNA Targets Leading to Allele-Specific Gene Expression and Contributing to Complex Disease Risk: A Systematic Review. *Public Health Genom.* **2020**, *23*, 155–170. [CrossRef]

131. Afrasiabi, A.; Fewings, N.L.; Schibeci, S.D.; Keane, J.T.; Booth, D.R.; Parnell, G.P.; Swaminathan, S. The Interaction of Human and Epstein-Barr Virus miRNAs with Multiple Sclerosis Risk Loci. *Int. J. Mol. Sci.* **2021**, *22*. [CrossRef] [PubMed]
132. Hassani, A.; Khan, G. Epstein-Barr Virus and miRNAs: Partners in Crime in the Pathogenesis of Multiple Sclerosis? *Front. Immunol.* **2019**, *10*, 695. [CrossRef] [PubMed]
133. Iizasa, H.; Kim, H.; Kartika, A.V.; Kanehiro, Y.; Yoshiyama, H. Role of Viral and Host microRNAs in Immune Regulation of Epstein-Barr Virus-Associated Diseases. *Front. Immunol.* **2020**, *11*, 367. [CrossRef]
134. Moyano, A.L.; Steplowski, J.; Wang, H.; Son, K.N.; Rapolti, D.I.; Marshall, J.; Elackattu, V.; Marshall, M.S.; Hebert, A.K.; Reiter, C.R.; et al. microRNA-219 Reduces Viral Load and Pathologic Changes in Theiler's Virus-Induced Demyelinating Disease. *Mol. Ther.* **2018**, *26*, 730–743. [CrossRef]
135. De Cock, A.; Michiels, T. Cellular microRNAs Repress Vesicular Stomatitis Virus but Not Theiler's Virus Replication. *Viruses* **2016**, *8*, 75. [CrossRef]
136. Campbell, T.; Meagher, M.W.; Sieve, A.; Scott, B.; Storts, R.; Welsh, T.H.; Welsh, C.J. The effects of restraint stress on the neuropathogenesis of Theiler's virus infection: I. *Acute disease. Brain Behav. Immun.* **2001**, *15*, 235–254. [CrossRef]
137. Welsh, C.J.; Tonks, P.; Nash, A.A.; Blakemore, W.F. The effect of L3T4 T cell depletion on the pathogenesis of Theiler's murine encephalomyelitis virus infection in CBA mice. *J. Gen. Virol.* **1987**, *68 Pt 6*, 1659–1667. [CrossRef] [PubMed]
138. Consortium. *; C.C. The genome architecture of the Collaborative Cross mouse genetic reference population. Genetics* **2012**, *190*, 389–401. [CrossRef]
139. Srivastava, A.; Morgan, A.P.; Najarian, M.L.; Sarsani, V.K.; Sigmon, J.S.; Shorter, J.R.; Kashfeen, A.; McMullan, R.C.; Williams, L.H.; Giusti-Rodriguez, P.; et al. Genomes of the Mouse Collaborative Cross. *Genetics* **2017**, *206*, 537–556. [CrossRef] [PubMed]
140. Kirby, A.; Kang, H.M.; Wade, C.M.; Cotsapas, C.; Kostem, E.; Han, B.; Furlotte, N.; Kang, E.Y.; Rivas, M.; Bogue, M.A.; et al. Fine mapping in 94 inbred mouse strains using a high-density haplotype resource. *Genetics* **2010**, *185*, 1081–1095. [CrossRef] [PubMed]
141. Morgan, A.P.; Fu, C.P.; Kao, C.Y.; Welsh, C.E.; Didion, J.P.; Yadgary, L.; Hyacinth, L.; Ferris, M.T.; Bell, T.A.; Miller, D.R.; et al. The Mouse Universal Genotyping Array: From Substrains to Subspecies. *G3 (Bethesda)* **2015**, *6*, 263–279. [CrossRef]
142. Blake, J.A.; Baldarelli, R.; Kadin, J.A.; Richardson, J.E.; Smith, C.L.; Bult, C.J.; Mouse Genome Database, G. Mouse Genome Database (MGD): Knowledgebase for mouse-human comparative biology. *Nucl. Acids Res.* **2021**, *49*, D981–D987. [CrossRef]
143. Keane, T.M.; Goodstadt, L.; Danecek, P.; White, M.A.; Wong, K.; Yalcin, B.; Heger, A.; Agam, A.; Slater, G.; Goodson, M.; et al. Mouse genomic variation and its effect on phenotypes and gene regulation. *Nature* **2011**, *477*, 289–294. [CrossRef] [PubMed]
144. Yalcin, B.; Wong, K.; Agam, A.; Goodson, M.; Keane, T.M.; Gan, X.; Nellaker, C.; Goodstadt, L.; Nicod, J.; Bhomra, A.; et al. Sequence-based characterization of structural variation in the mouse genome. *Nature* **2011**, *477*, 326–329. [CrossRef]